FH Aachen | Campus Jülich
Faculty of Chemistry and Biotechnology
Master in Nuclear Applications

RADIATION DAMAGE AND SUSTAINABILITY OF VANADIUM AND COPPER TARGET UNDER PROTON IRRADIATION USING MONTE CARLO SIMULATIONS

Master Thesis by

Syed, Mubashar Hassan

June 2026

This work has been supervised by

Dr. -Ing. Johannes Baggemann

Prof. Dr. phil. nat. Christoph Langer

Declaration of Authorship

I hereby declare that this thesis was completed independently and that all sources used have been properly acknowledged and referenced. Any passages taken directly or indirectly from published or unpublished works have been identified accordingly. This thesis has not been presented to any other examination authority and has not been published.

______________________ ______________________

Place, Date Signature

Acknowledgements

First of all, I would like to thank Dr. -Ing. Johannes Baggemann for giving me the opportunity to work on this project and also for his great supervision, motivation and help throughout my project, and for giving so much of his time and effort for our discussions.

Also, I would like to thank Prof. Dr. phil. nat. Christoph Langer for his support and guidance throughout my master's degree and invaluable feedback throughout the research process.

I would also like to thank the members of the JCNS-HBS group at Forschungszentrum Jülich, for their additional support, ideas and pleasant working atmosphere.

I am profoundly grateful to my family, especially my mother, whose unwavering love and relentless prayers have been the cornerstone of my journey. Their sacrifices and support have fueled my determination and inspired me to push through every challenge. I also extend my heartfelt thanks to my friends, whose belief in me has been a source of strength. This work would not have been possible without their boundless support and motivation.

Abstract

This thesis examines proton-induced radiation damage and sustainability of vanadium and copper-based target materials for High Current Accelerator-driven Neutron Source (HiCANS) applications, especially in the context of the High-Brilliance neutron Source (HBS) project at Forschungszentrum Jülich. Vanadium has been evaluated for 20 MeV proton irradiation target and copper is assessed for 3 MeV proton irradiation target or backing. The general objective is to estimate the amount of primary damage, the rate of damage accumulation and estimate the service life of the respective irradiation conditions.

Monte Carlo simulations have been carried out with SRIM/TRIM in full-cascade mode. Three different threshold displacement energy E_d cases were considered for each material; lower case, mean case, and upper case. The red line signifies the most likely estimate of damage E_d, and the lower and upper bounds indicate the range of uncertainty. The outputs from SRIM were translated into damage rates to include target displacement per ion (DPI) and damage distribution by depth (DDD) using NRT-dpa methodology, proton flux, atomic number density and full-power-year operation assumptions.

The results indicate that the spatial distribution and intensity of damage from radiation exposure are sensitive to proton energy, material density, proton stopping behaviour and the value of E_d. The proton penetration depth and distributed damage accumulation are deeper for Vanadium under 20 MeV proton irradiation and the annual damage rates have been calculated and used for estimation of service life of the target. Copper under 3 MeV irradiation shows damage concentrated closer to the near-surface region, which is significant for local degradation and replacement considerations. According to the literature, ductility retention and hydrogen compatibility of vanadium and vanadium alloys are relatively good, and copper should be carefully evaluated due to the sensitivity to irradiation hardening/hydrogen degradation and concerns with blistering.

Overall, the thesis investigates a methodology for radiation-damage evaluation of targets for accelerator-driven neutron source applications using SRIM/TRIM, for future target design purposes.

Contents

List of Figures

List of Tables

List of Abbreviations

CANS	Compact Accelerator-driven Neutron Source
HiCANS	High Current Accelerator-driven Neutron Source
HBS	High-Brilliance neutron Source
SRIM	Stopping and Range of Ions in Matter
TRIM	Transport of Ions in Matter
NRT	Norgett–Robinson–Torrens
arc-dpa	Athermal recombination-corrected displacements per atom
dpa	Displacements per atom
FPY	Full power year
PKA	Primary knock-on atom
MC	Monte Carlo
BCC	Body-centred cubic crystal structure
FCC	Face-centred cubic crystal structure
MeV	Mega electron volt
keV	Kilo electron volt
eV	Electron volt
V	Vanadium
Cu	Copper
E_d	Threshold displacement energy
E_p	Incident proton energy
N	Atomic number density
N_A	Avogadro constant
$\dot{N}_p$	Proton rate / number of protons per second
n_{disp}	SRIM target displacements per incident ion
φ	Particle flux

Φ	Particle fluence
ρ	Material density
M	Molar mass
d	Averaging depth or target thickness used in damage-rate calculation
A	Irradiated beam area
I	Beam current
e	Elementary charge
P	Beam power
t_{FPY}	Duration of one full power year
t_{life}	Estimated target service life
$\dot{d}_{pa}$	Damage rate expressed in dpa per second
T_{dam}	Damage energy available for atomic displacement production

1 Introduction and Research Background

1.1 HiCANS Technology and High-Brilliance Neutron Source Project

Over the past two decades, compact accelerator-based neutron sources (CANS) have been developed as complementary neutron-producing facilities alongside research reactors and large spallation sources. More recently, High Current Accelerator-driven Neutron Sources (HiCANS) have emerged as an advanced class of compact neutron sources intended to provide high neutron brilliance using high-current proton accelerators below the spallation threshold [1,2]. In this energy regime, neutrons are produced mainly through proton-induced nuclear reactions in a neutron-emitting target rather than through high-energy spallation.

The High-Brilliance neutron Source (HBS) is the German HiCANS project under development at Forschungszentrum Jülich. The HBS concept uses a high-current linear proton accelerator with proton energies in the 20–70 MeV range, combined with optimized target, moderator, and reflector systems, to generate neutron beams for scientific applications [1,2]. The target assembly is therefore a central component of the facility because it receives the incident proton beam directly and experiences the highest local irradiation and thermal loading.

In contrast to a fission reactor, neutron generation in an accelerator-driven source can be stopped by switching off the proton beam. This provides operational controllability and reduces some of the facility-level challenges associated with reactor-based neutron production [1]. However, this advantage does not remove the need for robust target design. The neutron-emitting target must remain structurally reliable under continuous proton bombardment, displacement damage, local energy deposition, gas production, and thermo-mechanical loading. The long-term sustainability of the target material is therefore one of the key technical questions in the HBS development.

Table 1.1 HiCANS and HBS context

Item	**Description**
Technology class	High Current Accelerator-driven Neutron Source
HBS role	German HiCANS project at Forschungszentrum Jülich
Typical proton-energy range	20–70 MeV, below the spallation threshold
Main target function	Neutron production through proton-induced nuclear reactions
Main material challenge	Maintaining target integrity under irradiation and thermal loading

1.2 Radiation Damage as a Target Material Challenge

When energetic protons penetrate a metallic target, they lose energy through electronic and nuclear interactions. Electronic stopping mainly contributes to ionization and heat generation, whereas nuclear stopping transfers kinetic energy directly to lattice atoms. If the transferred energy exceeds the threshold displacement energy, ED, atoms can be displaced from their lattice sites and vacancy–interstitial defects can be produced [3,4]. These primary displacement events can initiate collision cascades and generate vacancies, interstitials, replacement collisions, and defect clusters.

Accumulated displacement damage gradually modifies the mechanical behaviour of the material. Irradiation hardening may increase the yield strength or hardness, but it can also reduce ductility and decrease the ability of the target to tolerate thermal stresses. Hydrogen and helium generated or implanted during irradiation can further contribute to embrittlement, bubble formation, or blistering. Therefore, the target lifetime depends not only on neutron-production performance but also on the evolution of material properties during long-term irradiation [3].

For this reason, target qualification requires a radiation-damage analysis that connects SRIM/TRIM simulation outputs to physically meaningful engineering quantities. In this thesis, the central damage quantity is the displacement per atom (*dpa*). The *dpa* value is used as a radiation-exposure measure and is later converted into annual damage accumulation and estimated service life using the calculation route introduced in Chapter 3.

The main calculation quantities used later in the thesis are introduced here to clarify the notation. Full numerical substitutions are given in Chapter 3.

$$N = \rho N_A / M \qquad (1.1)$$

where N is the atomic number density, ρ is the material density, N_A is Avogadro's constant, and M is the molar mass.

$$\varphi = \dot{N}_p / A \qquad (1.2)$$

where φ is the proton flux, $\dot{N}_p$ is the number of incident protons per second, and A is the irradiated target area.

$$\Phi = \varphi t \qquad (1.3)$$

where Φ is the proton fluence accumulated during irradiation time t.

$$dpa/FPY = \dot{d}_{pa} \times t_{FPY} \qquad (1.4)$$

where $\dot{d}_{pa}$ is the damage rate in dpa s^{-1} and t_{FPY} is the number of seconds in one full power year. Detailed derivations and numerical substitutions are presented in Chapter 3.

Symbol	Meaning	Unit
E_d	Threshold displacement energy	eV
N	Atomic number density	atoms cm^{-3} or atoms Å^{-3}
N_A	Avogadro constant	mol^{-1}
φ	Proton flux	protons cm^{-2} s^{-1} or protons Å^{-2} s^{-1}
Φ	Proton fluence	protons cm^{-2}
$\dot{N}_p$	Number of incident protons/s	protons s^{-1}
$\dot{d}_{pa}$	Damage rate	dpa s^{-1}
t_{FPY}	Time corresponding to one full power year	s
dpa/FPY	Annual displacement damage	dpa per full power year

Table 1.2. Main degradation mechanisms relevant for HBS target materials

Mechanism	**Target consequence**
Displacement damage	Generation of vacancies, interstitials, and defect clusters
Irradiation hardening	Increase in strength or hardness with possible loss of ductility
Hydrogen effects	Embrittlement, bubble formation, or blistering
Swelling or void formation	Dimensional instability and reduction of mechanical integrity
Thermo-mechanical loading	Stress accumulation due to beam-induced heating and cooling cycles

1.3 Materials Investigated in This Thesis

This thesis investigates two materials used in different HBS-related irradiation scenarios. Vanadium is considered for a 20 MeV proton-irradiated target concept, whereas copper is considered for a 3 MeV proton-irradiated target, backing, or diagnostic application. The two materials are not treated as direct competitors for the same target design. Instead, each material is assessed under its own relevant proton-energy condition and application context.

The selection of vanadium is motivated primarily by its strong neutron yield at 20 MeV proton energy and its relevance to HBS neutron-emitting target concepts. In addition, vanadium offers favourable activation behaviour, a body-centred cubic crystal structure, and promising radiation tolerance. Literature studies indicate that vanadium and V–4Cr–4Ti-type alloys can retain useful ductility at significant accumulated damage levels while showing relatively limited swelling and favourable hydrogen transport behaviour [5–11]. For this reason, vanadium requires a quantified damage-rate and service-life assessment under the 20 MeV HBS-related irradiation condition.

Copper is considered because of its role as a backing plate and support material for the lithium target concept. In this configuration, the thin lithium foil does not fully stop the incident proton beam; instead, a significant part of the proton beam penetrates through the lithium layer and stops inside the copper backing. Therefore, the radiation tolerance of copper must be investigated under the relevant 3 MeV proton irradiation condition, however proton beam loose its energy due to nuclear reactions in lithium layer and stopped by copper backing plate at 1.3 MeV. Copper is also attractive because of its excellent thermal conductivity, which supports heat removal from the lithium layer and helps prevent lithium melting during operation. However, copper can show irradiation-induced hardening, defect formation, hydrogen-related blistering, and ductility loss under proton irradiation conditions [12–15]. For this reason, copper sustainability must be evaluated carefully rather than assuming that its thermal advantages alone guarantee long service life.

Table 1.3Materials and irradiation scenarios considered in this thesis

Material	Irradiation scenario	Assessment Reason	Main concern
Vanadium	20 MeV proton-irradiated target concept	Strong neutron yield, activation behaviour, and promising radiation tolerance	Damage accumulation and service-life limit
Copper	3 MeV proton-irradiated target/backing or diagnostic concept	Excellent thermal conductivity and engineering relevance	Hardening, hydrogen blistering, and ductility loss

1.4 Research Gap

Although radiation damage in metals has been investigated extensively, the proton-energy regime relevant to HiCANS and HBS target applications is less developed than the literature for conventional reactor and fusion irradiation environments. Many available studies focus on a single material response, such as irradiation hardening, hydrogen permeation, blistering, swelling, or ductility degradation. These studies are valuable, but they do not by themselves provide a complete target service-life assessment for the specific HBS-related irradiation cases.

A second gap is methodological. SRIM/TRIM simulations provide displacement-related outputs such as target displacements per ion, but they do not directly provide a final service life. The simulation output must be combined with beam parameters, target area, atomic number density, and the selected threshold displacement energy, ED, to calculate the damage rate and annual accumulated dpa. The mean ED value gives the most representative damage estimate, while lower and upper ED values provide an uncertainty range [4].

The present thesis addresses these gaps by using the same SRIM/TRIM-based calculation route for both irradiation scenarios. Vanadium is assessed for the 20 MeV case and copper for the 3 MeV case. The results are interpreted with reference to published mechanical-property and hydrogen-behaviour data, so that the calculated damage rate can be linked to material sustainability and expected service life.

1.5 Aim and Objectives of the Present Thesis

The main aim of this thesis is to quantify proton-induced radiation damage, calculate damage accumulation rates, and evaluate the expected service life of vanadium and copper under their respective HBS-related irradiation conditions using SRIM/TRIM-based methodology.

The specific objectives are:

- To quantify primary displacement damage in vanadium under 20 MeV proton irradiation and copper under 3 MeV proton irradiation using SRIM/TRIM Monte Carlo simulations.
- To calculate damage rates and annual accumulated damage doses in *dpa*/*FPY* from SRIM target-displacement outputs.
- To determine the sensitivity of the calculated damage rate to lower, mean, and upper threshold displacement energy values, E_d.
- To evaluate the expected service life of each material under its own irradiation scenario.
- To interpret the calculated damage levels using published literature on irradiation hardening, ductility retention, hydrogen compatibility, blistering, and microstructural stability.

Table 1.4 Research objectives of the thesis

Objective	Description
1	Quantify SRIM/TRIM displacement damage
2	Calculate damage rate and dpa/FPY
3	Evaluate E_d uncertainty using lower, mean, and upper values
4	Determine service life for each material scenario
5	Interpret results using irradiation-response literature

1.6 Scope and Limitations

This thesis is limited to primary proton-induced displacement damage and its interpretation in relation to target sustainability. The computational work uses SRIM/TRIM full-cascade simulations and post-processing of target-displacement outputs to calculate damage rates and *dpa*/*FPY*. The analysis includes sensitivity to E_d but does not include fully coupled thermal-mechanical or gas-diffusion modelling.

The thesis does not perform coupled thermal-mechanical finite-element modelling, direct experimental post-irradiation testing, or explicit secondary neutron-damage transport calculations. Long-time defect migration, cascade overlap at very high fluence, and full gas-diffusion modelling are also outside the direct scope. These effects are discussed as limitations and future work, but the primary calculation framework remains the SRIM/TRIM-based proton damage assessment.

Table 1.5 Scope of the present investigation

Included	Excluded
Primary proton-induced displacement damage	Explicit secondary neutron-damage transport calculation
SRIM/TRIM full-cascade simulations	Coupled thermal-mechanical finite-element analysis
ED sensitivity study	Experimental post-irradiation examination
Damage rate and dpa/FPY calculation	Long-time defect diffusion and gas-transport simulation
Service-life interpretation using literature data	Full economic optimization of target replacement

1.7 Structure of the Thesis

This thesis is organized as follows. Chapter 2 introduces the theoretical background of primary radiation damage, the displacement-per-atom concept, threshold displacement energy, and the SRIM/TRIM framework. Chapter 3 describes the investigated materials, beam assumptions, simulation setup, and the calculation procedure used to convert SRIM outputs into damage rates and service-life estimates. Chapter 4 presents the simulation results for the vanadium 20 MeV and copper 3 MeV irradiation cases, including the lower, mean, and upper E_d scenarios. Chapter 5 discusses the results in relation to published radiation-response literature and evaluates the service-life implications for each material. Chapter 6 summarizes the main conclusions and identifies future work required for target qualification.

2 Theoretical Background

Chapter scope clarification: this chapter provides the theoretical basis for SRIM/TRIM-based proton-induced displacement-damage calculations and for the subsequent service-life estimation of the vanadium 20 MeV target and the copper 3 MeV target concept. The two materials are not treated as interchangeable candidates for one identical target, but as two separate HBS-related target cases evaluated using the same calculation methodology.

2.1 Displacement Damage Physics

Radiation damage of metallic target materials starts when energetic particles impart kinetic energy on atoms of the crystal lattice. Radiation of the proton beam in proton irradiated targets is dissipated in two significant processes: electronic and nuclear stopping. Electronic stopping transfers energy directly to electrons, and leads to ionization and heat production, whereas nuclear stopping directly transfers energy to the atomic nuclei with collisions. It is only the nuclear component of the deposited energy that can produce permanent atomic displacements in the lattice and hence is the most significant component in primary radiation damage analysis [18,19].

At elevations of transferred recoil energy greater than the threshold displacement energy of the material, the struck atom will be able to depart its equilibrium lattice site. The initial knock-on atom is often referred to as the primary knock-on atom (PKA). Assuming that the PKA possesses sufficient energy, it can create additional displacements (by a series of second collisions). Such a sequence is referred to as a cascade of displacement. The cascade can generate vacancies, interstitials, replacement collisions and small clusters of defects, dislocation loops and local regions of high atomic disorder [16,17,21].

In the case of proton-driven neutron-source targets, the damage caused by the primary radiation is not a single microscopic phenomenon. The fact that displacement damage accumulates during long periods of operation makes it an engineering problem since repeated proton irradiation produces displacement damage. With an increase in the density of radiation generated defects, there is a transformation in the microstructure, and mechanical characteristics like hardness, yield strength, ductility, fracture behavior and resistance to swelling may vary. The sustainability of a target material is thus directly proportional to the displacement damage accumulation rate, and the capability of the material to retain useful mechanical properties with the resulting damage dose [21,24,25].

Formation of primary damage has a very short time scale. The ballistic phase of a displacement cascade occurs on the order of femtoseconds to picoseconds. Once this has occurred, a significant proportional number of displaced atoms will have the ability to recombine without being thermally activated via long-range diffusion. This is referred to as athermal recombination. This is one of the reasons that instantly displaced atoms did not have the same number as the surviving defects after the cascade cools [20,21]. This difference is significant to this thesis since the dpa values calculated are not directly relied upon as a radiation exposure measure, and to draw comparisons between vanadium and copper, rather than as an absolute measure of end-resultant defect concentration.

Table 2.1 Key concepts in primary displacement damage.

Concept	Meaning in this thesis
Electronic stopping	Energy transfer to electrons; mainly ionization and heat
Nuclear stopping	Energy transfer to nuclei; responsible for atomic displacements
PKA	Primary knock-on atom created after a collision event
Frenkel pair	Vacancy and interstitial pair produced by displacement
Cascade	Sequence of collisions initiated by a PKA
Athermal recombination	In-cascade recombination of vacancies and interstitials

2.2 Displacements per Atom as Damage Exposure Parameter

Single displacements per atom, dpa, is the most commonly used measure of quantities used to compare radiation damage. Any value of dpa is defined as the average form of the number of times each atom in the volume of interest has been moved by the designated displacement model. A dpa value of 0.01 corresponds to one atom out of a hundred being displaced, on average. The dpa concept proves handy as it normalizes damages to the number of atoms in the material hence permitting comparison of various targets, particle energies and irradiation circumstances [17,21].

The displacement-per-atom value is calculated from the number of displaced target atoms normalized to the number of atoms in the same considered volume:

$$\mathrm{dpa} = N_{disp} / N_{atoms} \qquad (2.1)$$

The atomic number density of a target material is calculated from density and molar mass:

$$N = \rho N_A / M \qquad (2.2)$$

Symbols used in Equations (2.1) and (2.2).

Symbol	**Meaning**	**Unit**
dpa	displacements per atom	dimensionless
N_{disp}	number of displaced atoms	atoms or displacements
N_{atoms}	number of atoms in the considered volume	atoms
N	atomic number density	atoms cm^{-3} or atoms $Å^{-3}$
ρ	mass density	g cm^{-3}
N_A	Avogadro constant	mol^{-1}
M	molar mass	g mol^{-1}
dpa	Displacements per atom	dimensionless
N_{disp}	Number of displaced target atoms	atoms or displacements
N_{atoms}	Number of atoms in the considered volume	atoms
N	Atomic number density	atoms/cm^3 or atoms/$Å^3$
ρ	Mass density	g/cm^3
N_A	Avogadro constant	mol^{-1}
M	Molar mass	g/mol

The practical benefit of dpa is that, at least physically, it is more important to the structural damage than proton fluence alone. Analyzing the same fluence can also have a variety of effects on different materials as the stopping power, recoil spectrum, atomic density and threshold displacement energy are not the same. Moreover, the same fluence and various proton energies may result in varying projected ranges and varying depth profiles. Hence, higher sustainability in targets is expected to be discussed in the terms of dpa rate and accumulated dpa as opposed to beam fluence alone [18,19,21].

At the same time, dpa must be interpreted carefully. According to the OECD/NEA review, the NRT-dpa has continued to be a valuable tool as a measure of damage exposure on a scaled basis, but should not be used as a precise measure of the number of defects that survive within metals [21]. It has been demonstrated shortly, both by calculations in molecular dynamics and experimental studies, that most defects generated in the early cascade phase recombine prior to any stable microstructure being generated. The thesis thus utilizes dpa as comparative and engineering metric of damage, the mechanical relevance of such damage is investigated based on literature on vanadium and copper irradiation response.

Table 2.2 Radiation-damage quantities and their relevance.

Quantity	Definition	Usefulness for target damage
Proton fluence	Number of incident protons per area	Does not include material response
Absorbed dose	Energy deposition per mass	Includes electronic energy not directly producing displacement
NRT-dpa	Standard displacement exposure parameter	Useful for comparison and first-order lifetime estimates
arc-dpa	Recombination-corrected damage measure	Requires correction parameters and additional processing

2.3 NRT-dpa Formalism

The NRT-dpa formalism is based on the earlier Kinchin–Pease displacement model and its later refinement by Norgett, Robinson and Torrens [16,17]. The model proposed by Kinchi-Pease incorporated a new idea that the atomic movements depend on the recoil energy that is accessible in damaging the nuclear. This relation was changed in the NRT model by adding a displacement efficiency factor and by taking into account the damage energy that can be used in the production of atomic displacement [17].

For recoil energies above the threshold region, the NRT estimate of the number of displacements is calculated as:

$$N_{d,NRT} = 0.8\, T_{dam} \,/\, (2E_d) \qquad (2.3)$$

This equation shows why E_d must be written and treated consistently: for the same damage energy, a lower E_d gives a higher displacement yield, while a higher E_d gives a lower displacement yield.

Symbol	Meaning	Unit
$N_{d,NRT}$	Number of NRT displacements produced by the recoil damage energy	displacements
T_{dam}	Damage energy available for atomic displacement production	eV
E_d	Threshold displacement energy	eV
0.8	NRT displacement efficiency factor	dimensionless

The NRT model is relevant since it is very basic, portable and has been extensively applied in the comparison of irradiation settings. It allows conversion of SRIM/TRIM outputs in average and peak rates of damage in target studies. Ophoven et al. used this technique on a tantalum target irradiated by 70 MeV protons and extracted SRIM displacement data and scaled by proton flux to calculate dpa/s and dpa per full power year [23]. The current thesis uses the identical conceptual workflow in reference to vanadium at 20 MeV and copper at 3 MeV.

The limitation of NRT-dpa is that it generally overestimates surviving defects in metals. This is because the NRT model does not consider enough in-cascade recombination, clustering, thermal spikes and subsequent defects evolution. However, it can still be applied to the current thesis since the objective is not to forecast all stable vacuity or interstitial. The objective is to compute a steady primary damage exposure, and contrast two target materials in the face of well-stated assumptions [19,21].

2.4 Arc-dpa Correction Methodology

Athermal-recombination-corrected dpa, abbreviated arc-dpa, was introduced to improve the physical realism of primary damage calculations in metals by accounting for in-cascade recombination. It can be expressed in simplified form as:

$$N_{d,arc} = \xi_{arc}(T_{dam})\, N_{d,NRT} \qquad (2.4)$$

Symbols used in Equations (2.3) and (2.4).

Symbol	Meaning	Unit
$N_{d,NRT}$	number of displacements predicted by NRT	displacements
$N_{d,arc}$	athermal-recombination-corrected displacements	displacements
T_{dam}	damage energy available for atomic displacement	eV
E_d	threshold displacement energy	eV
ξ_arc(T_dam)	arc-dpa defect-production efficiency factor	dimensionless
Symbol	Meaning	Unit
$N_{d,arc}$	Athermal-recombination-corrected displacement estimate	displacements
ξ_arc(T_dam)	Damage-energy-dependent defect production efficiency	dimensionless
$N_{d,NRT}$	NRT displacement estimate	displacements

The arc-dpa model has theoretical significance in that it explicitly acknowledges that the number of defects that end up stationary is less than the NRT number of displacements. Nordlund et al. stressed that better atomic displacement models must be able to differentiate between displaced atoms, surviving defects and atom replacements since they are physically different [20]. Owing to this fact, arc-dpa is becoming a more popular parameter used to measure primary defect production in metals than the uncorrected NRT-dpa [20,21,36].

Nevertheless, the benefit of arc-dpa does not make it the main calculation metric in this thesis. There are three reasons. First, the SRIM/TRIM workflow in the present case is based on the standard one-HBS-relevant damage-processing scheme where SRIM displacement results are transformed into NRTs-type damages rates [23]. Second, NRT-dpa is the most commonly used exposure measure, and that is appropriate to be compared with the published thresholds of damages. Third, accurate material-specific arc-dpa parameterization adequate across all instances and target geometries is not always easy. Thus, NRT-dpa is indicated as primary finding and arc-dpa is considered as an invaluable limitation and a future improvement.

Table 2.3 Position of NRT-dpa and arc-dpa in this thesis.

Model	Physical meaning	Use in this thesis
NRT-dpa	Standard damage exposure	Main metric used in thesis
arc-dpa	Corrected surviving defect estimate	Discussed as limitation/future improvement
Replacement per atom	Atom relocation/mixing measure	Not calculated in this thesis

2.5 Threshold Displacement Energy

The threshold displacement energy E_d is the lowest possible recoil energy to dislodge an atom at its lattice site and form a steady defect. It is among the most sensitive parameters of material in the calculation of displacement damages. When the recoil energy is less than E_d, the atom can vibrate and get back to its original state. When the recoil energy is greater than E_d, a stable vacuity interstitial pair can be formed [21,22].

The energy of the threshold displacement is not a characteristic single fixed constant at the atomic level. It is based on crystal direction, local binding, temperature, and probability of defect recombination. A direction in a crystalline material can require less energy to be displaced than another direction due to the difference between the local atomic environment. For engineering calculations, an averaged threshold displacement energy is therefore used. Konobeyev et al. compared averaged energy loss of threshold displacement and associated data of numerous elements including copper and vanadium [22].

For this thesis, the averaged threshold displacement energy values are taken as 30 ± 6 eV for copper and 57 ± 11 eV for vanadium [22]. These values are entered in the SRIM/TRIM target setup as the displacement energy E_d for the corresponding material. The mean value is treated as the most probable input, while the lower and upper values define the uncertainty range used for the sensitivity study.

Table 2.4 Threshold displacement energy cases used in SRIM/TRIM simulations.

Material	**Lower E_d**	**Average E_d**	**Upper E_d**
Copper	24 eV	30 eV	36 eV
Vanadium	46 eV	57 eV	68 eV

2.6 SRIM/TRIM and Binary Collision Approximation

A popular program for computing ion transport, stopping power, range distributions and radiation-damage related quantities in solids is its Stopping and Range of Ions in Matter (SRIM) [18]. TRIM, which is the Transport of Ions in Matter module, is a Monte Carlo model of ion-transport simulations that tracks incident ions and recoil atoms as they pass through a target. It employs the binary collision approximation, where ion and recoil atom interactions are represented by a series of two-body interactions [18,19].

Ion trajectories, projected ranges and much of primary collision-event quantities are well-calculated with the binary collision approximation. Nevertheless, it is unable to entirely model many-body effects within thick cascades, thermal spikes, long-time diffusion, defect motion, or temperature little microstructural growth. SRIM/TRIM is thus to be interpreted as a means of estimating the primary damage exposure and not a full- blown model of ultimate mechanical degradation [19,21].

Stoller et al. gave guidance on the use of SRIM for radiation-damage exposure calculations and emphasized that the user must clearly identify which SRIM output is used [19]. In this thesis, the SRIM/TRIM output used for subsequent damage-rate calculation is the target displacement yield, i.e., target displacements per incident ion, together with the depth-dependent displacement profile. The SRIM output itself is not a final dpa rate; it is converted into dpa/s and dpa/FPY by the post-processing equations in Chapter 3.

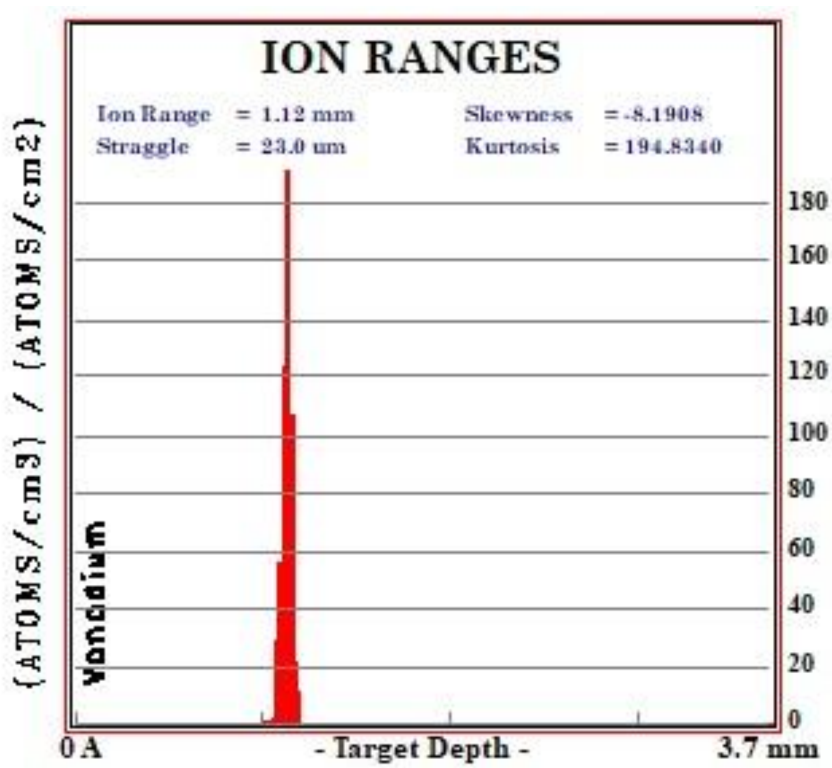

Figure 2.1 Representative SRIM/TRIM ion range output from the vanadium 20 MeV proton simulation set used for this thesis.

The practical meaning of the theoretical range concept is shown in the representative SRIM/TRIM output in Figure 2.1.

Figure 2.1 is used here to connect the theoretical discussion of ion range to the practical SRIM output. The range distribution shows where the 20 MeV protons slow down and stop in the vanadium target. This is important because the damage rate is not uniform through the full target thickness; it follows the depth-dependent stopping and recoil-production behaviour.

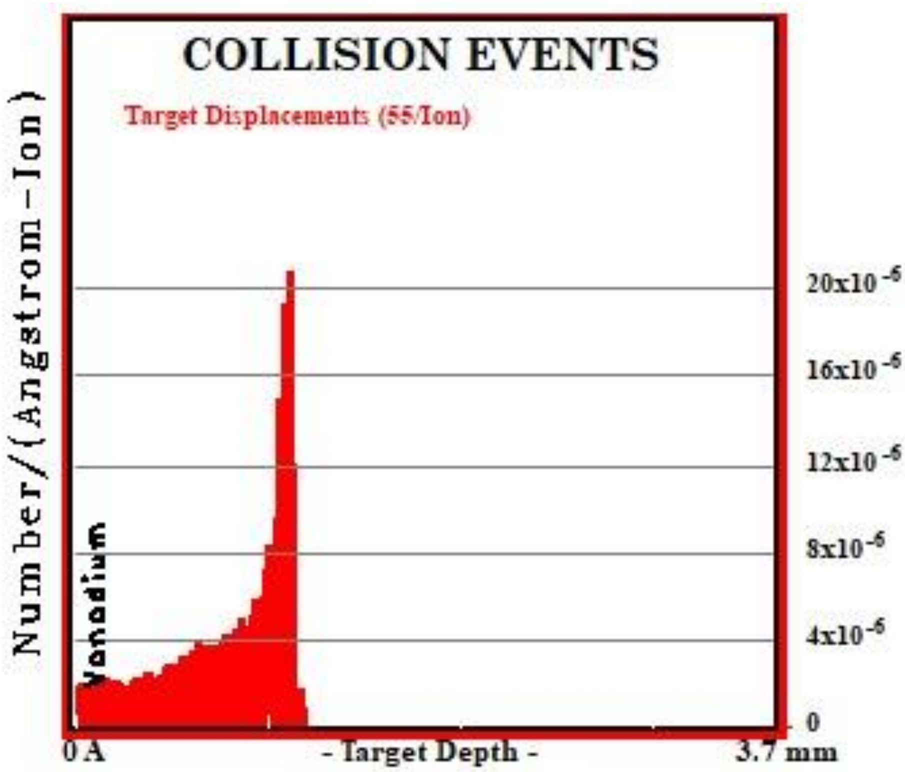

Figure 2.2 Representative SRIM/TRIM collision-events output from the vanadium simulation package. Collision-event data are used for post-processing damage-rate calculations

The collision-event output used for damage-rate post-processing is shown in Figure 2.2.

Figure 2.2 illustrates the type of collision-event information required for the subsequent calculation. The target-displacement output is extracted from SRIM/TRIM and then inserted into the damage-rate formula. Therefore, the figure is not only illustrative; it identifies the SRIM result that becomes the numerical input for the dpa calculation.

2.7 Literature-Based Radiation Response of Vanadium for the 20 MeV Proton Target Application

Vanadium is a body-centred-cubic metal considered here for the separate 20 MeV proton target case. It is selected because HBS-related target development includes a vanadium target concept for this energy range and because literature reports favourable radiation tolerance, ductility retention and hydrogen transport behaviour in vanadium and V–4Cr–4Ti alloys [27–31].

Irradiation hardening in vanadium and V–4Cr–4Ti alloys is expected because displacement defects obstruct dislocation motion. The key however is that hardening does not necessarily imply loss of target usability. It has been published in literature on V-4Cr-4Ti that when it is irradiated strength can be enhanced and useful ductility is maintained even at relatively high damage levels [30,31]. This renders vanadium unlike copper where hardening can be accompanied by a nanosecond ductility degradation in the presence of hydrogen [32].

Hydrogen behavior is central to proton target sustainability. Malo et al. measured the permeation of deuterium with the help of vanadium and obtained high temperature dependence, which shows that at high temperature, the hydrogen transport becomes an even more favourable one [27]. Su et al. demonstrated that first-principles calculations found that to form hydrogen bubbles in vanadium, substantial vacancy stabilization is needed, indicating that alone accumulated hydrogen is insufficient to form a catastrophic bubble in bulk vanadium [28].

Blistering caused by helium and gases simply cannot be overlooked. Kaletta demonstrated that the temperature dependence of blistering of vanadium by helium was severe as higher temperatures tended to be less toxic to blisters which became more toxic in lower temperature regions [29]. As such, vanadium cannot be said to be immune to gas effects. It can be better explained as a material that has a good hydrogen transportation and increased resistance to the formation of hydrogen bubbles as compared to copper.

Table 2.5 Theoretical relevance of vanadium for HBS target analysis.

Parameter	**Vanadium**
Crystal structure	BCC
Average Ed used	57 eV
Main benefit	Hydrogen compatibility and ductility retention
Main concern	Damage accumulation and gas effects at long operation
Advanced candidate	V–4Cr–4Ti alloy

2.8 Literature-Based Radiation Response of Copper for the 3 MeV Proton Target Application

Copper is a face-centred-cubic metal considered here for the separate 3 MeV target/backing concept. It is selected because copper is technically relevant for low-energy target assemblies owing to its high thermal conductivity and engineering availability; however, its radiation response must be assessed carefully because irradiation hardening, hydrogen blistering and ductility loss are reported in the literature [32–35].

Kiener et al. demonstrated that single-crystal copper irradiated with protons can exhibit high strengthening at small sizes and strong defect-obstacle benefits [32]. Irradiation in copper often generates stacking fault tetrahedra and defect structures that limit the motion of dislocations. This hardens the material but it removes the plastic deformation capacity of the material. Lower plasticity may escalate the danger of brittle or intergranular failure in a target component that is subjected to thermal gradients.

The primary drawback of proton environments on copper is Hydrogen damage. Hydrogen may accumulate at defects or near surfaces or at grain boundaries. Sznajder et al. talked about hydrogen blistering at extreme radiation environments and they demonstrated that the process of blistering is a multifaceted relationship among hydrogen inventory, defects and temperature [33]. Even more recent accelerator-material experiments describe blistering issues in various copper alloys when subjected to hydrogen ion environment [34]. The observations suggest that copper may be useful in either replaceable or backing applications, but must be cautioned against direct long-term operation under proton-imposed hydrogen loading.

In the current thesis, copper is thus assessed not only based on its computed dpa rate, but also based on its the literature informed susceptibility to hydrogen degradation. The difference is significant, since two materials of similar elastic stiffness may exhibit radically different target lifetimes when one is ductile and one is brittle in its fracture behavior.

Table 2.6 Theoretical relevance of copper for HBS target analysis.

Parameter	Copper
Crystal structure	FCC
Average E_d used	30 eV
Main benefit	High thermal conductivity and engineering familiarity
Main concern	Hardening, ductility loss, hydrogen blistering
Likely target role	Backing, heat sink, replaceable or sacrificial component

2.9 Summary of Theoretical Basis

The chapter provided the theoretical foundation on calculation of radiation-damage and material sustainability analysis used in this thesis. Lattice damage is caused by proton irradiation which occurs due to nuclear collisions and displacement cascades. The caused damage is measured by the dpa concept. Primary exposure is characterized by the NRT-dpa formalism and arc-dpa is covered as a more sophisticated correction method that considers athermal recombination.

Critical parameters of sensitivity include the threshold displacement energy. Copper and vanadium are thus modeled by lower, intermediate and upper E_d values. SRIM/TRIM delivers ion range/displacement-event data, but post-processing these data with beam flux, target depth/atomic number density gives the ultimate damage rates and lifetime estimates.

The theoretical basis therefore supports two separate service-life assessments. Vanadium is evaluated for the 20 MeV proton target case, and copper is evaluated for the 3 MeV target/backing case. The same SRIM/NRT calculation chain is used for both cases, but the results must be interpreted against the material-specific literature and the intended target function rather than as a simple material competition.

3 Materials and Simulation Parameters

3.1 Target Material Properties

This chapter outlines the material properties, simulation setup, flux calculations and damage-rate approach used for the separate evaluation of the vanadium 20 MeV proton target and the copper 3 MeV target/backing case. The simulations were performed in SRIM/TRIM using hydrogen ions as incident protons and the material-specific threshold displacement energies described in Chapter 2.

The damage-rate requires the material properties of density, molar mass, atomic number density, crystal structure and threshold displacement energy. The atomic number density depends on the density and molar mass, and is found in the denominator of the dpa-rate equation. A higher atomic number density means that the same number of displacements is distributed over more atoms, reducing the calculated dpa for a given displacement yield.

Vanadium and copper have different density, atomic mass, crystal structure and target function. Vanadium is treated as the 20 MeV target material, while copper is treated as the 3 MeV target/backing material. The common purpose of the calculation is not to choose one universal material, but to estimate the damage rate and service life for each material under its corresponding irradiation condition.

Table 3.1 Target materials and basic properties used for simulation and calculation.

Material	Atomic number	Molar mass (g/mol)	Density (g/cm³)	Crystal structure	Proton energy
Vanadium	23	50.94	6.11	BCC	20 MeV
Copper	29	63.55	8.96	FCC	3 MeV

3.2 Experimental and Beamline Context

The quantitative aspect of this thesis is founded on SRIM/TRIM simulations and post-processing analytical dpa-rate. The experimental photographs in this chapter capture information of the beamline, target environment and target-component context within which the material study is located. The photos are taken as contextual records of the

HBS-related experimental context and target-development facilities; they are not considered as separate mechanical test outcomes.

Photographs of the accelerator hall reveal the shielded beamline and target-area setting. The dense shielding blocks, beamline components, detector/diagnostic apparatus and target-manipulation apparatus evidences the engineering, in practice, limitations related to small accelerator-driven neutron-source target work. The target should be not only designed to meet the nuclear performance, but should also achieve cooling, accessibility, alignment, shielding and replacement.

Close-up shots of the machined part of the target indicate a metallic channeled framework. Channel geometries are important since thermal management is a target-design objective. Coupling High local power density and irradiation damage are not only simultaneous, but also necessitate a concerted effort to couple cooling geometry and material radiation response in subsequent design phases. In the current thesis, however, thermal-hydraulic characteristics of the channel geometry are not modeled; attention is on primary displacement damage and sustainability through dpa. The corresponding figure is introduced here because it is directly used to support the methodological statement in this section.

Figure 3.1 Machined target/cooling-channel component documented during the facility visit. The channelled geometry illustrates the importance of thermal management in target design.

Figure 3.1 documents the accelerator hall and target-area environment. It supports the methodological description by showing that the simulated target cases correspond to a real shielded beamline setting rather than an isolated numerical exercise.

The corresponding figure is introduced here because it is directly used to support the methodological statement in this section.

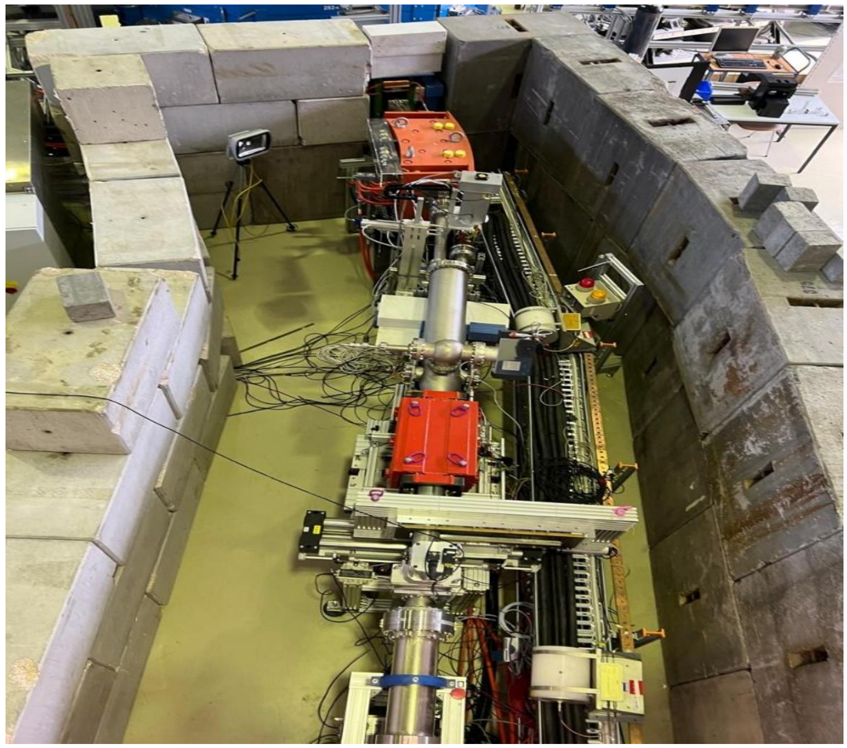

Figure 3.2 Shielded accelerator/beamline area showing target-area constraints and surrounding experimental infrastructure.

Figure 3.2 further shows the spatial constraints around the shielded beamline. These constraints are relevant because target design, cooling channels and diagnostics must be compatible with the available experimental infrastructure.

Figure 3.3. Beamline and target-area environment documented during the experimental facility visit. The photograph provides context for the target-irradiation infrastructure used in HBS-related work

The corresponding figure 3.3 is introduced here because it is directly used to support the methodological statement in this section.

Figure 3.3 shows a machined target/cooling-channel component. This figure is included to emphasize why the damage calculation is linked to sustainability: irradiation damage occurs in a component that must also remove heat and preserve mechanical integrity.

3.3 SRIM/TRIM Simulation Configuration

SRIM/TRIM was modeled to run on vanadium and copper. Both cases had a hydrogen/proton as the incident ion. Incidence was assumed to be normal, i.e. 0 degrees to the target surface normal. In the case of vanadium, the energy of protons was 20 MeV. In case of copper, the proton energy was 3 MeV. The quantity of simulated ions was to be 15 000, which corresponds to the practical tradeoff between the statistical reliability and the computational time employed in HBS-based work related to SRIM [23].

The mode of full damage cascade calculation is the right mode to be used in this thesis, as the aim is to get collision-event and displacement data. Quick calculation modes lack the detailed displacement-damage evaluation due to their lack of the entire recoil cascade representation. Outputs of the simulation thus involve ion range, collision records, displacement of target, vacancies, replacement collision, phonon, ionization and energy deposition files.

Three simulations were being carried out with lower, average and upper threshold displacement energy values of the corresponding material. The threshold displacement energy was entered in the SRIM/TRIM target setup window. The output target displacements of individual run are used to get the beginning point of the dpa-rate calculations. Three E_d cases are required due to the uncertainty of the evaluated threshold displacement energies, and the inverse relationship between damage production and E_d [22].

Table 3.2: SRIM/TRIM simulation configuration used in this thesis.

Parameter	**Vanadium simulation**	**Copper simulation**
Ion type	H^+ / proton	H^+ / proton
Ion energy	20 MeV	3 MeV
Incidence angle	0°	0°
Number of ions	15,000	15,000
Calculation mode	Detailed/full cascade	Detailed/full cascade
E_d cases	46, 57, 68 eV	24, 30, 36 eV

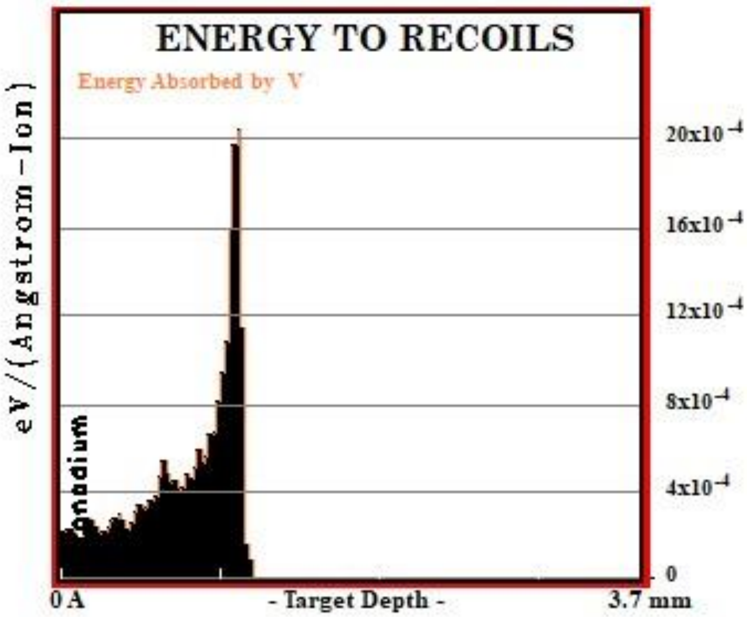

Figure 3.4 Representative SRIM/TRIM energy absorption output from the vanadium 20 MeV simulation set.

The corresponding figure is introduced here because it is directly used to support the methodological statement in this section. Figure 3.4 is a representative SRIM/TRIM energy-deposition output. It is used to verify that the simulation records the depth-dependent beam interaction and provides the physical basis for later displacement and damage-rate calculations.

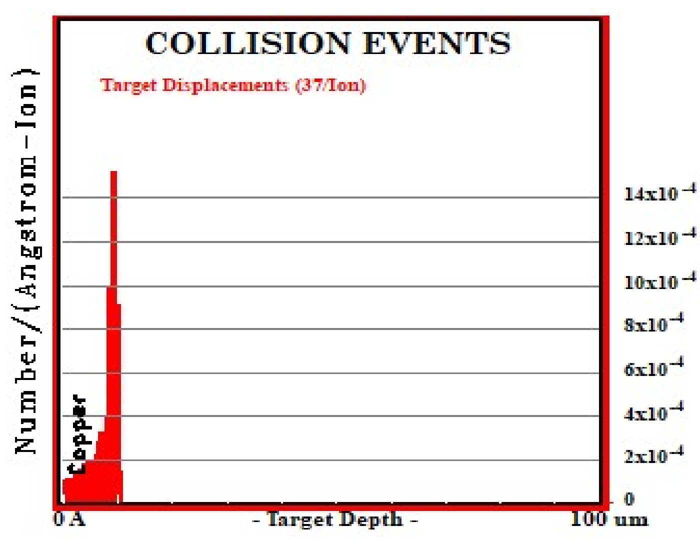

Figure 3.5 Representative SRIM/TRIM output from the 3 MeV copper simulation set.

The corresponding figure is introduced here because it is directly used to support the methodological statement in this section.

Figure 3.5 is a representative copper 3 MeV simulation output. It supports the methodology by showing the lower-energy copper case separately from the 20 MeV vanadium case.

3.4 Threshold Displacement Energy Sensitivity Study

One of the main methodological aspects of this thesis is the threshold displacement energy sensitivity study. One E_d would provide a single estimate of damage-rate and would conceal a significant source of uncertainty. Konobeyev et al. state the values of averaged threshold displacement energies with uncertainty values of both target materials [22]. These values were converted into lower, average, and upper SRIM/TRIM input cases.

For copper, the average value is 30 eV with an uncertainty of ±6 eV, giving 24 eV, 30 eV and 36 eV simulation cases. For vanadium, the average value is 57 eV with an uncertainty of ±11 eV, giving 46 eV, 57 eV and 68 eV simulation cases. The unit of the NRT relation is such that the magnitude of displacements decreases with the increase in E_d. As such, it could be presumed that the lower E_d case would yield the maximum calculated damage rate and that the upper E_d case would yield the minimum calculated damage rate.

Table 3.2 Ed sensitivity cases and expected influence on displacement yield.

Case	Value	Interpretation
Copper lower E_d	24 eV	Expected highest Cu displacement yield
Copper average E_d	30 eV	Baseline Cu case
Copper upper E_d	36 eV	Expected lowest Cu displacement yield
Vanadium lower E_d	46 eV	Expected highest V displacement yield
Vanadium average E_d	57 eV	Baseline V case
Vanadium upper E_d	68 eV	Expected lowest V displacement yield

3.5 Fluence and Flux Calculation

To convert SRIM/TRIM displacement yield into a damage rate, the incident proton rate, proton flux and atomic density must first be calculated. Flux and fluence are different quantities and are used differently in this thesis: flux is used for damage rate, whereas fluence is used for accumulated damage over a defined irradiation time.

$$E_p = E_{MeV} \times 1.602 \times 10^{-13}\ \mathrm{J} \quad (3.1)$$

$$\dot{N}_p = P / E_p \quad \text{or} \quad \dot{N}_p = I / e \quad (3.2)$$

$$\varphi = \dot{N}_p / A \quad (3.3)$$

$$\Phi = \varphi t \quad (3.4)$$

$$N = \rho N_A / M \quad (3.5)$$

Symbols used in Equations (3.1)–(3.5).

Symbol	**Meaning**	**Unit**
E_p	energy of one incident proton	J
E_{MeV}	proton kinetic energy used in SRIM/TRIM	MeV
$\dot{N}_p$	incident proton rate	protons s^{-1}
P	beam power	W
I	beam current	A
e	elementary charge	C
A	irradiated target area	cm^2 or $Å^2$
φ	proton flux	protons cm^{-2} s^{-1} or protons $Å^{-2}$ s^{-1}
Φ	proton fluence	protons cm^{-2} or protons $Å^{-2}$
t	irradiation time	s
N	atomic number density	atoms cm^{-3} or atoms $Å^{-3}$
Symbol	Meaning	Unit
E_p	Energy of one incident proton	J/proton
E_{MeV}	Proton kinetic energy	MeV

Symbol	Meaning	Unit
N_dot	Number of incident protons per second	protons/s
P	Beam power	W = J/s
I	Beam current	A = C/s
e	Elementary charge, 1.602 × 10^−19	C
A	Irradiated beam area	cm² or Å²
φ	Proton flux	protons/cm²/s
F	Proton fluence	protons/cm² or protons/Å²
t	Irradiation time	s
N	Atomic number density	atoms/cm³ or atoms/Å³

The proton flux φ is a rate per unit area. It must not be confused with fluence Φ. In the present calculation chain, φ is inserted into the damage-rate equation, while Φ would be used only if accumulated damage after a specified irradiation time is calculated directly.

For the vanadium 20 MeV calculation check, the beam-loading case used a proton energy of 20 MeV, a beam power of 80 kW and an irradiated area of 15 cm × 15 cm = 225 cm². This gives a proton rate of approximately 2.50 × 10^16 protons/s and a flux of approximately 1.11 × 10^14 protons/cm²/s, equivalent to 0.0111 protons/Å²/s. The vanadium atomic density used in the calculation is 7.22 × 10^22 atoms/cm³, equivalent to 0.0722 atoms/Å³.

Vanadium calculation check used in this thesis.

For the 20 MeV vanadium case, the calculation uses $P = 80$ kW, $A = 225$ cm², $\varphi \approx 1.11 \times 10^{14}$ protons cm^{-2} s^{-1} = 0.0111 protons Å^{-2} s^{-1}, $N \approx 7.22 \times 10^{22}$ atoms cm^{-3} = 0.0722 atoms Å^{-3}, and $I = 4$ mA. The resulting annual damage values are reported as 10.76 dpa FPY^{-1} for $E_d = 46$ eV, 7.33 dpa FPY^{-1} for $E_d = 57$ eV, and 5.76 dpa FPY^{-1} for $E_d = 68$ eV.

The mean E_d case gives the most probable damage rate and therefore the most probable service-life estimate. The lower and upper E_d cases define the uncertainty band: lower E_d produces a conservative higher damage estimate, while upper E_d produces a lower damage estimate.

Table 3.3 Flux and atomic-density equations used before dpa-rate calculation.

Vanadium E_d case	**E_d value**	**Calculated annual damage**
Lower E_d	46 eV	10.76 dpa/FPY
Mean E_d	57 eV	7.33 dpa/FPY
Upper E_d	68 eV	5.76 dpa/FPY
Quantity	**Value**	**Unit**
Proton energy, E_p	20	MeV
Beam power, P	80	kW
Irradiated area, A	225	cm^2
Proton rate, N_dot	2.50 × 10^16	protons/s
Flux, φ	1.11 × 10^14	protons/cm^2/s
Flux, φ	0.0111	protons/$Å^2$/s
Vanadium atomic density, N	7.22 × 10^22	atoms/cm^3
Vanadium atomic density, N	0.0722	atoms/$Å^3$
Quantity	**Equation**	**Purpose**
Proton energy	Ep = E(MeV) × 1.602 × 10^−13 J	Converts MeV to joules
Proton rate from power	Ndot = P/Ep	Used when beam power is specified
Proton rate from current	Ndot = I/e	Used when beam current is specified
Flux	φ = Ndot/A	Protons /unit area/s
Atomic density	N = ρNA/M	Atoms per unit volume

3.6 Damage-Rate Calculation Method

The radiation-damage calculations in this thesis were performed using the SRIM/TRIM Monte Carlo simulation package. The quantity extracted from SRIM was the number of target displacements produced by each incident proton. Following the SRIM-based methodology of Ophoven et al., the average damage rate was calculated from the SRIM output using Equation (3.1).

$$R_d = \frac{n_{disp} \cdot \varphi}{d \cdot N} \tag{3.6}$$

The variables used in Equation (3.6) are defined in Table below. The use of this equation makes clear which SRIM output was used and how the result was converted into a damage rate.

Symbol	Meaning	Unit
R_d	Average damage rate	dpa s^{-1}
n_{disp}	The value of n_{disp} was obtained from the SRIM/TRIM target-displacement output. For average damage-rate calculations, the displacement value was averaged over the selected penetration or target depth, whereas for peak damage-rate calculations, the maximum displacement value from the depth-resolved SRIM profile was used.	displacements ion^{-1}
φ	Proton flux	ions cm^{-2} s^{-1}
d	Target thickness or averaging depth	cm
N	Atomic number density	atoms cm^{-3}

For depth-dependent or peak damage calculations, the local displacement production was determined from the depth-resolved SRIM output using Equation (3.7).

$$R_d(z) = \frac{n_{disp}(z) \cdot \varphi}{N} \tag{3.7}$$

In Equation (3.7), the term $n_{disp}(z)$ represents the local target displacement production at the depth position z. This form was used only for interpreting the peak-damage region and the depth-resolved SRIM damage profiles.

The annual damage accumulation was calculated by multiplying the damage rate by one full power year, as shown in Equation (3.8).

$$dpa/FPY = R_d \cdot t_{FPY} \tag{3.8}$$

The duration of one full power year was taken as continuous operation for 365 days:

$$t_{FPY} = 365 \times 24 \times 3600 = 3.1536 \times 10^7\ s \qquad (3.9)$$

The estimated target service life was then calculated by dividing the allowable displacement-damage limit by the annual damage accumulation.

$$t_{life} = \frac{dpa_{limit}}{dpa/FPY}$$

(3.10)

The calculation sequence was therefore: SRIM target displacements per ion → damage rate in dpa s^{-1} → annual damage in dpa/FPY → estimated service life. The complete handwritten substitutions are kept in the calculation appendix, while the main thesis reports the equations, input quantities, units, and final calculated values.

For the vanadium target, the calculated annual damage values were obtained for the three threshold displacement energy cases listed in Table below.

Case	Threshold displacement energy	Annual damage
Lower uncertainty case	E_d = 46 eV	10.76 dpa/FPY
Mean case	E_d = 57 eV	7.33 dpa/FPY
Upper uncertainty case	E_d = 68 eV	5.76 dpa/FPY

The mean E_d value represents the most probable estimate of target damage. The lower and upper E_d values are not alternative operating choices; they provide an uncertainty range for the calculated damage rate and predicted service life.

3.7 Simulation Output Handling

It is installed on the simulation package with single folders of vanadium 20 MeV target and copper 3 MeV target. The vanadium set comprises of the first simulation, maximum-threshold simulation and minimum-threshold simulation folders. The copper set also has the baseline, maximum-threshold as well as the minimum-threshold simulation folders. and on each of these folders are SRIM/TRIM output files like TRIMIN, VACANCY, PHONON, IONIZ, STOPPING and associated bitmap plots.

The collision-event or target-displacement output is the primary SRIM result used for the damage-rate calculation. Vacancy plots and ionization plots are useful for physical interpretation, but the numerical post-processing uses target displacements per incident ion, because this value is directly compatible with Equations (3.6) and (3.7).

The presence of the bitmap plots in simulation folders can be used to provide visual evidence of the depth dependence of proton penetration and energy deposition. The range of protons in the case of vanadium (20 MeV) is considerably greater compared with that in copper (3 MeV). As a result, the distribution of the vanadium damage is deeper in the target, and the copper case is more located closer to the surface. That difference is significant as the local severity of damage can be enhanced with near-surface concentration, which raises the risk of hydrogen accumulation and blistering.

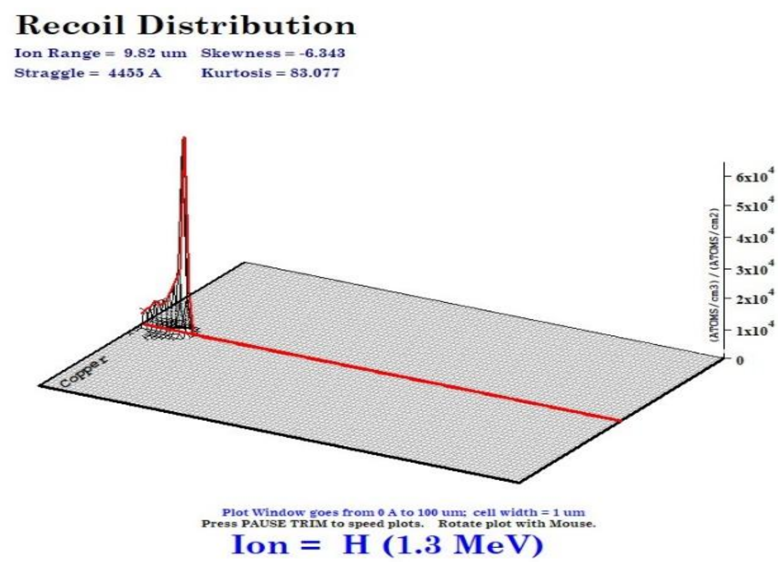

Figure 3.6 Additional representative SRIM/TRIM result from the 3 MeV copper simulation set, used for checking depth-dependent damage behavior.

The corresponding figure is introduced here because it is directly used to support the methodological statement in this section, and it illustrates the SRIM/TRIM interpretation of incident proton beam 1.3 MeV, considering loss of energy due to nuclear reactions in lithium layer.

Figure 3.6 is used as a qualitative check of the depth-dependent copper damage behaviour. The output confirms that the 3 MeV case must be interpreted through a near-surface/local damage profile rather than only by whole-target averaging.

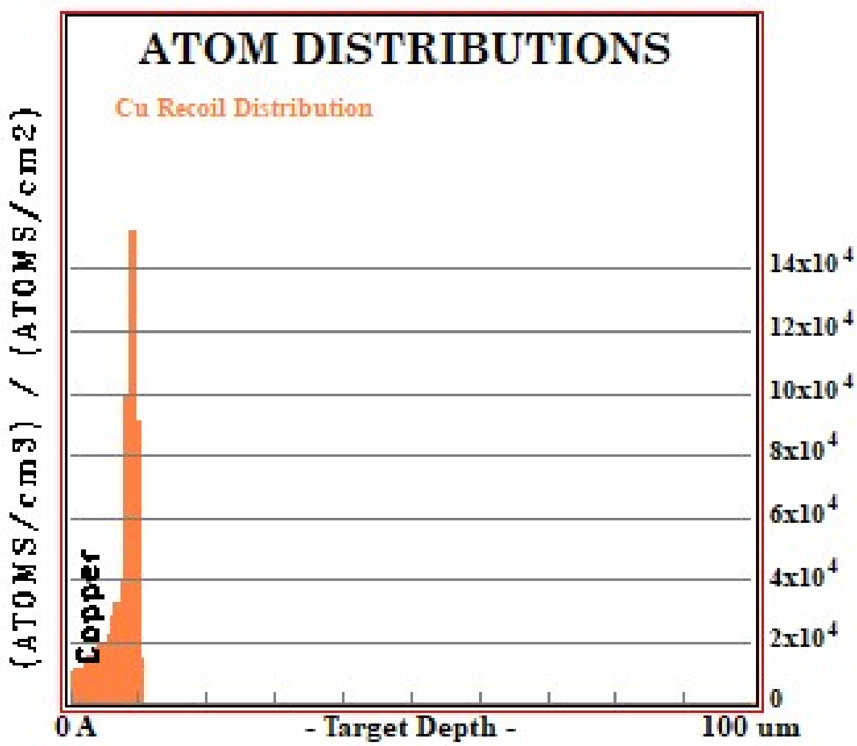

Figure 3.7 Representative copper simulation output used to support qualitative interpretation of the 3 MeV damage profile.

Figure 3.7 provides an additional copper simulation output used to support the 3 MeV target/backing analysis. The figure is included after the output-handling section because it directly relates to how SRIM plots are selected and interpreted.

Copper calculation check used in this thesis.

For the 3 MeV copper case, the calculation uses $P = 4.86$ kW, $\varphi \approx 0.11889$ protons Å^{-2} s^{-1}, $N = 0.08453$ atoms Å^{-3}, and $I = 1.62$ mA. The resulting annual damage values are reported as 47.63 dpa FPY^{-1} for $E_d = 24$ eV, 36.03 dpa FPY^{-1} for $E_d = 30$ eV, and 28.23 dpa FPY^{-1} for $E_d = 36$ eV.

The mean E_d case gives the most probable damage rate and therefore the most probable service-life estimate. The lower and upper E_d cases define the uncertainty band: lower E_d produces a conservative higher damage estimate, while upper E_d produces a lower damage estimate.

3.8 Assumptions and Limitations of the Methodology

The current methodology has several assumptions. First, SRIM/TRIM calculation specifies the primary proton-induced displacement damage but does not specifically model the secondary neutron damage. Second, there is no thermal-mechanical coupling or temperature-dependent diffusion, or hydrogen transport kinetics; and long-time defect evolution is omitted. Third, the target is not represented based on a three-dimensional finite-element model of the target; rather, simplified material and beam parameters are used that are appropriate to dpa calculation.

These constraints are acceptable for the present stage because the aim is to estimate proton-induced primary damage rates and service lives for each target case. The results should therefore be interpreted as first-stage sustainability estimates. Experimental irradiation, post-irradiation mechanical testing, coupled thermal-mechanical modelling and possible arc-dpa refinement remain necessary future steps.

A further limitation is the uncertainty in E_d and in SRIM's binary collision approximation. The first uncertainty is to some degree covered by the E_d sensitivity study. The second uncertainty is addressed by the fact that clearly SRIM/TRIM is a primary-damage tool, but not a whole-material-degradation model. This interpretation is guided by SRIM radiation-damage experimentation, and the NEA primary radiation damage framework [19,21].

Table 3.4 Methodological limitations and future extension routes.

Issue	Treatment in this thesis	Implication
Secondary neutron damage	Not explicitly calculated	Discussed as future improvement
Thermal-mechanical stress	Not modelled	Requires FEM coupling
Hydrogen diffusion	Not simulated	Interpreted using literature
arc-dpa correction	Not primary output	Future refinement
Experimental property testing	Not performed in thesis	Needed for qualification

3.9 Link to Results and Sustainability Assessment

The technique outlined in this chapter generates the numerical framework of Chapter 4. The SRIM/TRIM simulations offer the target displacement results and profile data according to depth in each material and E_d case. These are translated into damage rates and yearly doses of displacement. The outcomes of both vanadium and copper are subsequently compared in terms of dpa accumulation, depth distribution and anticipated life span.

The sustainability evaluation is not based only on dpa/FPY. After the service life is calculated, the accumulated dpa must be interpreted with literature data on mechanical-property change. For vanadium this means considering hardening, ductility retention and hydrogen transport. For copper this means considering irradiation hardening, hydrogen blistering and possible ductility loss. This link between calculated service life and expected material-property change is the basis of the discussion chapter.

4 Results and Analysis

This chapter presents the SRIM/TRIM simulation results and the derived radiation-damage calculations for the two target cases investigated in this thesis: vanadium irradiated by 20 MeV protons and copper irradiated by 3 MeV protons. The results follow the calculation workflow introduced in Chapter 3. The SRIM/TRIM outputs are first described using the ion range, energy-loss, recoil and displacement plots. The displacement yield obtained from SRIM/TRIM is then converted into an annual damage accumulation in dpa/FPY and into a first-order service-life estimate.

The chapter is organized in two separate material-specific parts because vanadium and copper refer to different HBS-related target situations. Vanadium is assessed for the 20 MeV neutron-emitting target case, where the proton penetration depth and damage distribution extend into a larger target volume. Copper is assessed for the 3 MeV target/backing or diagnostic case, where the lower incident proton energy produces a shallower near-surface damage region. The results are therefore not used to decide which material should replace the other, but to determine the expected radiation-damage accumulation and service-life implications for each material in its own irradiation scenario.

4.1 Vanadium 20 MeV Proton Irradiation

4.2 SRIM Simulation Outputs

The vanadium simulations were performed in the full-cascade configuration of SRIM/TRIM for incident protons with an initial energy of 20 MeV. The relevant outputs for the damage analysis are the ion distribution, range statistics, energy-loss curves, recoil distributions and target-displacement plots. The quantity used directly in the damage-rate calculation is the SRIM/TRIM target-displacement yield, expressed as target displacements per incident proton. In the interpretation below, the term dpa is used as an exposure quantity and not as the actual number of stable defects remaining after cascade recombination.

The 20 MeV proton case produces a deeper ion range than the 3 MeV copper case because proton range increases strongly with incident kinetic energy. Consequently, the vanadium damage profile is not restricted to an extremely thin surface layer.

Instead, the SRIM/TRIM output shows a depth-dependent displacement distribution inside the target. The relevant quantities to distinguish are the proton penetration depth, the depth of the displacement profile and the position of the maximum damage distribution; these are related but not identical.

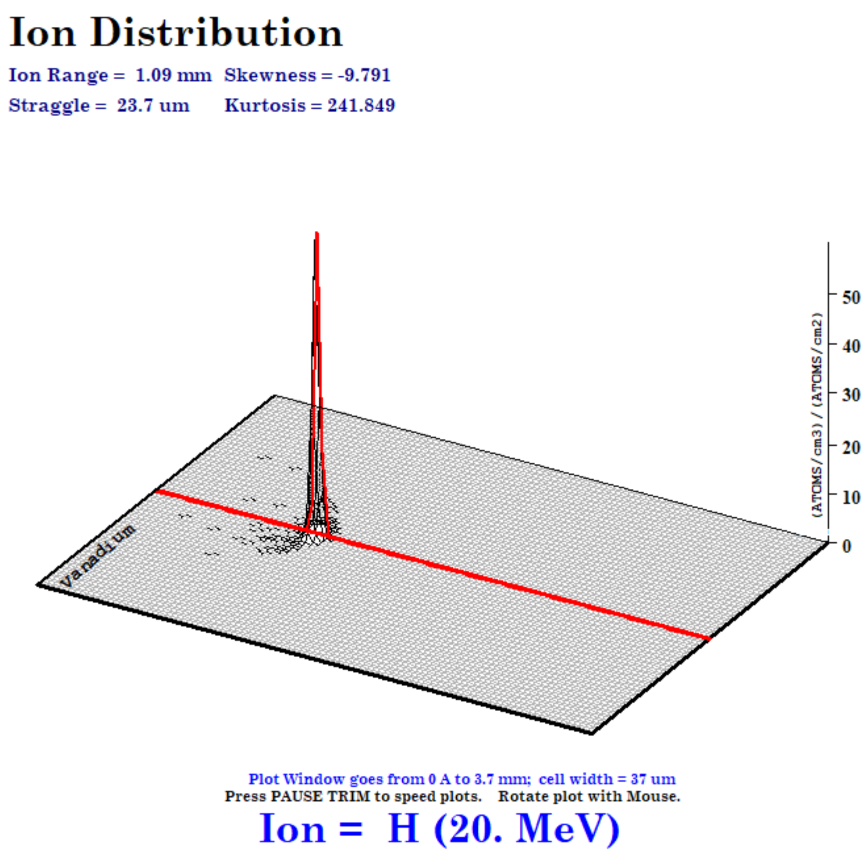

Figure 4.1 SRIM/TRIM ion distribution for 20 MeV proton irradiation of vanadium

The figure 4.1 shows the longitudinal and lateral distribution of the simulated protons and provides the basis for identifying the stopping region of the incident particles inside the target.

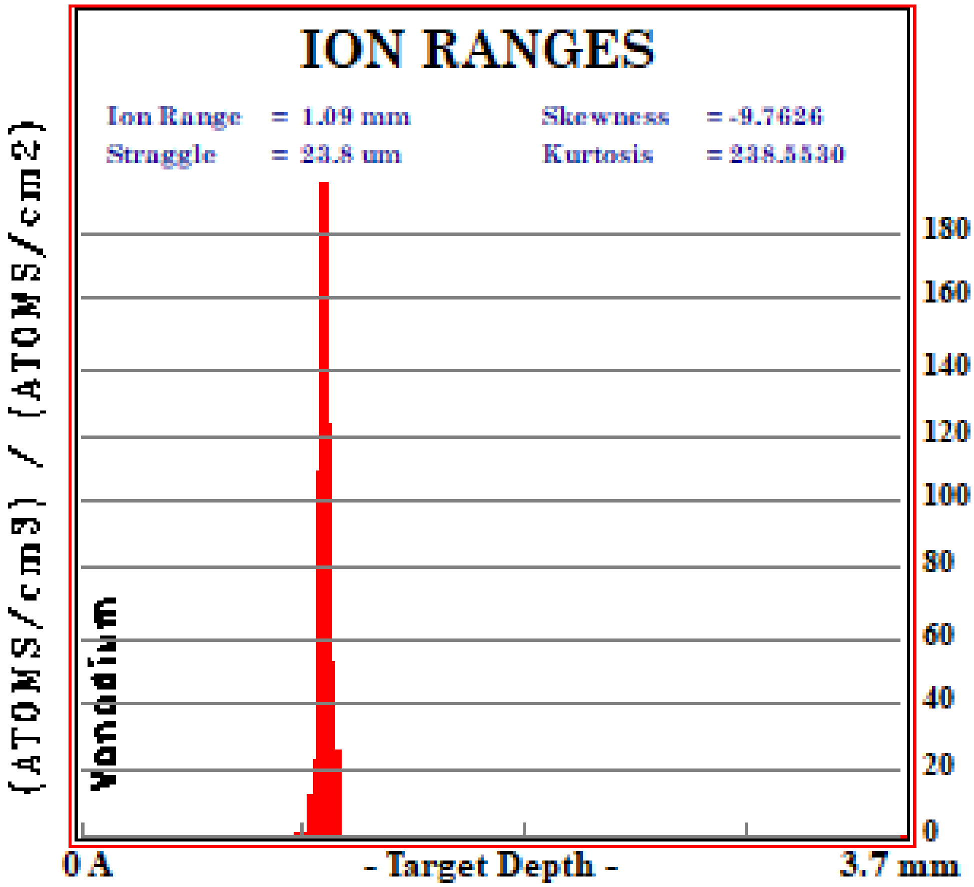

Figure 4.2 Ion-range output for 20 MeV protons in vanadium.

The range distribution confirms that the 20 MeV proton beam penetrates substantially into the vanadium target. This figure 4.2 is used only to describe the proton stopping distribution; the displacement profile is evaluated separately using the SRIM/TRIM radiation-damage output.

4.3 Proton Range and Damage Distribution

The ion-range output indicates that 20 MeV protons penetrate a significant distance into the vanadium target before stopping. This behavior is expected because proton penetration depth increases with incident kinetic energy. For HBS target analysis, the important point is that the region of maximum damage is located below the immediate surface and must be considered together with the surrounding depth distribution. Therefore, both average damage and local peak damage are relevant for service-life assessment.

The energy-loss outputs separate electronic and nuclear stopping contributions. Electronic stopping is the dominant energy-loss channel for the slowing down of high-energy protons, but it primarily excites or ionizes electrons and subsequently contributes to heat generation. It is not treated as direct displacement damage in the NRT-dpa calculation. Nuclear stopping, by contrast, transfers energy directly to lattice atoms and is responsible for creating primary knock-on atoms and displacement cascades. Therefore, only displacement-related SRIM/TRIM outputs are used for the damage-rate calculation.

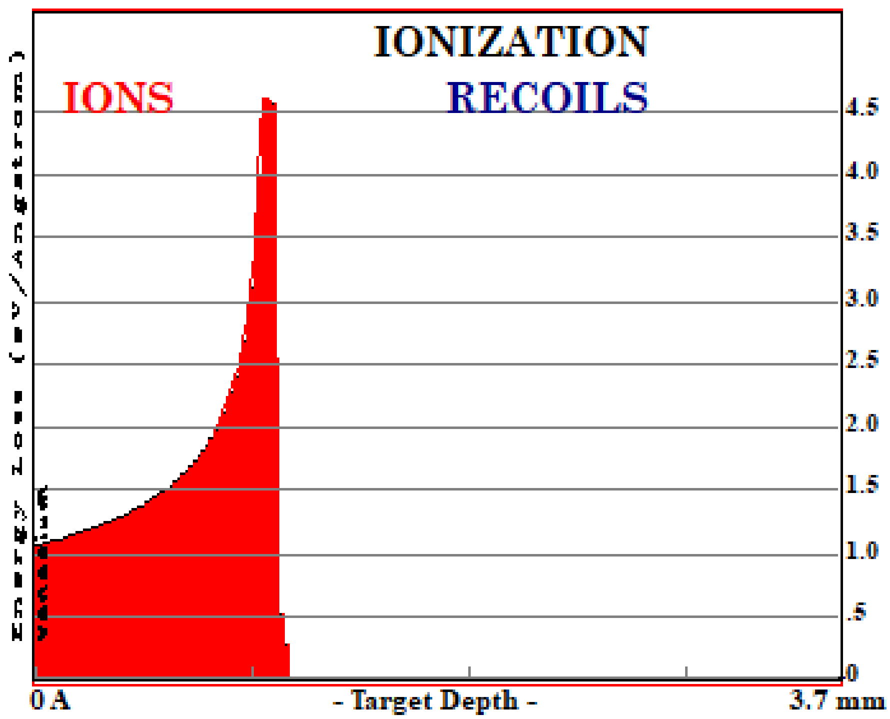

Figure 4.3 Energy-loss output for 20 MeV protons in vanadium

In fig 4.3 the curve distinguishes electronic energy loss from nuclear collision processes. Electronic stopping contributes mainly to excitation, ionization and heat, whereas nuclear stopping is directly relevant for atomic displacements.

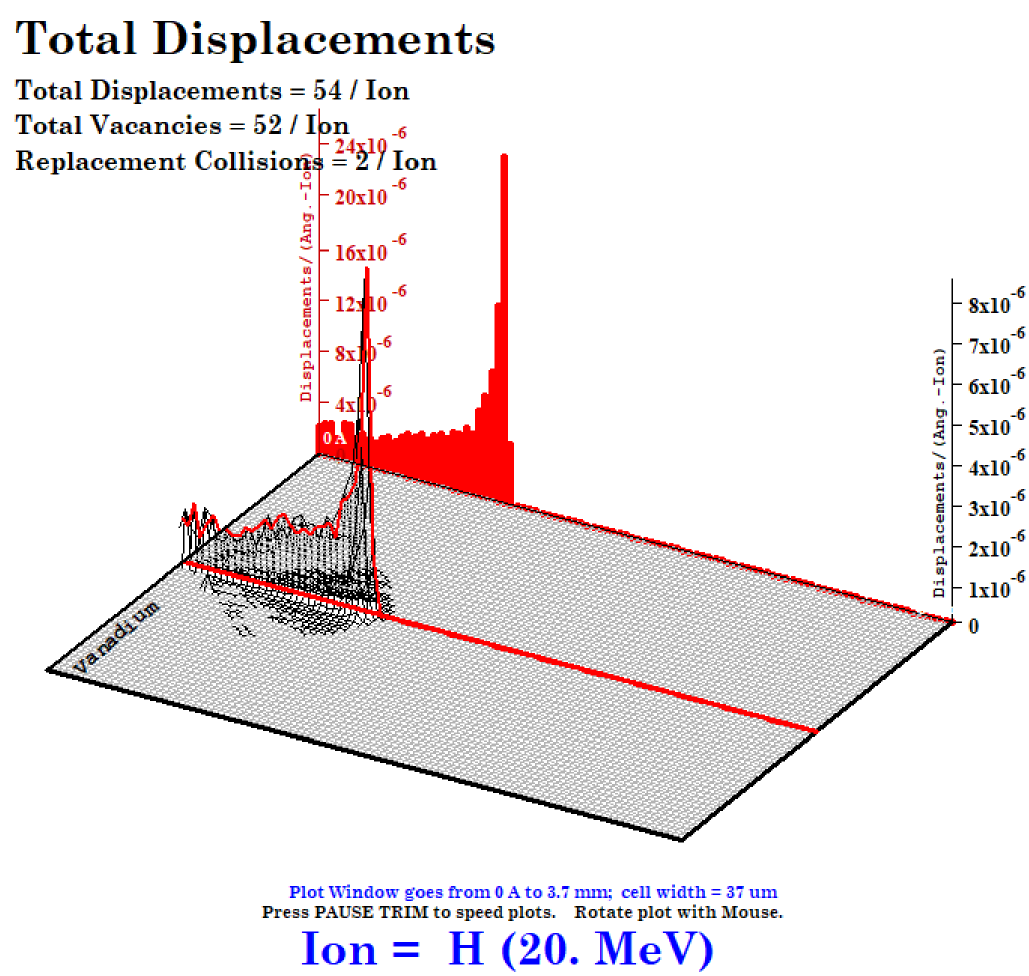

Figure 4.4 Depth-resolved radiation-damage profile for 20 MeV proton irradiation of vanadium.

The figure 4.4 identifies the region where displacement production is highest and therefore indicates the local part of the target expected to experience the strongest irradiation-induced property changes.

4.4 Displacement Yield for Lower, Average, and Upper E_d

The threshold displacement energy E_d is one of the main parameters controlling the number of displacements calculated by SRIM/TRIM. For vanadium, the evaluated average threshold displacement energy is 57 eV with an uncertainty of approximately ±11 eV [42]. Therefore, three vanadium cases were evaluated: a lower E_d case of 46 eV, an average E_d case of 57 eV and an upper E_d case of 68 eV. The average value is treated as the representative case, while the lower and upper values define an uncertainty range.

The lower and upper E_d cases are not technical measures for reducing or increasing damage in an operating target. They are sensitivity cases in the simulation model. A lower E_d means that recoil events are more likely to exceed the displacement threshold and therefore generate more calculated atomic displacements. A higher E_d means that fewer recoil events exceed the threshold and the calculated displacement production decreases. The resulting spread in annual dpa/FPY is therefore interpreted as model uncertainty in the radiation-damage estimate.

Table 4.1 Threshold displacement energy cases used for the 20 MeV vanadium simulations.

Vanadium case	Threshold displacement energy E_d	Relative displacement expectation	Interpretation
Lower evaluated E_d	46 eV	Highest	Conservative high-damage case
Average E_d	57 eV	Reference	Representative case
Upper E_d	68 eV	Lowest	Lower-damage sensitivity case

4.5 Damage Rate Calculations

The methodology introduced in Chapter 3 was used to convert the SRIM/TRIM displacement yield into a damage rate. The calculation uses the target-displacement yield per incident proton, the proton flux, the atomic number density of vanadium and the selected averaging depth. For vanadium, the atomic number density calculated from density and molar mass is approximately 7.22×10^{22} atoms cm^{-3}. Using the beam parameters and the SRIM/TRIM displacement yield, the calculated annual damage accumulation is reported in dpa/FPY.

For the average E_d case, the calculated annual damage accumulation is approximately 7.33 dpa/FPY. The upper E_d case gives a lower annual damage accumulation of approximately 5.76 dpa/FPY, while the lower E_d case gives a higher annual damage accumulation of approximately 10.76 dpa/FPY. These values show that the uncertainty in E_d has a significant influence on the calculated vanadium damage rate, but the resulting service-life estimate remains in the multi-year range for the first-order 30 dpa threshold used in this thesis.

Table 4.2 Calculated annual damage accumulation for 20 MeV proton irradiation of vanadium.

Vanadium E_d case	Calculated annual damage	Relative severity	Use in assessment
46 eV	10.76 dpa/FPY	Highest	Conservative lifetime estimate
57 eV	7.33 dpa/FPY	Reference	Main reported case
68 eV	5.76 dpa/FPY	Lowest	Upper-threshold sensitivity estimate

4.6 Depth-Resolved Damage Profiles

The depth-resolved damage distribution indicates that the displacement damage in vanadium is not uniform along the target depth. The maximum of the damage distribution occurs in a localized region associated with increased nuclear interactions and recoil production. This result shows why both average and local damage quantities are useful: the average dpa supports a first-order service-life estimate, whereas the peak region identifies the part of the target most likely to experience local mechanical-property changes.

The lateral spread shown by the SRIM/TRIM output indicates that the beam footprint and the spatial distribution of the incident proton flux influence the local damage field. In a real target, beam spot size, beam rostering, cooling geometry and target thickness all affect whether damage remains localized or is distributed over a larger volume. These design-dependent effects are not explicitly simulated here, but the SRIM/TRIM profiles provide the primary damage distribution needed for first-order sustainability assessment.

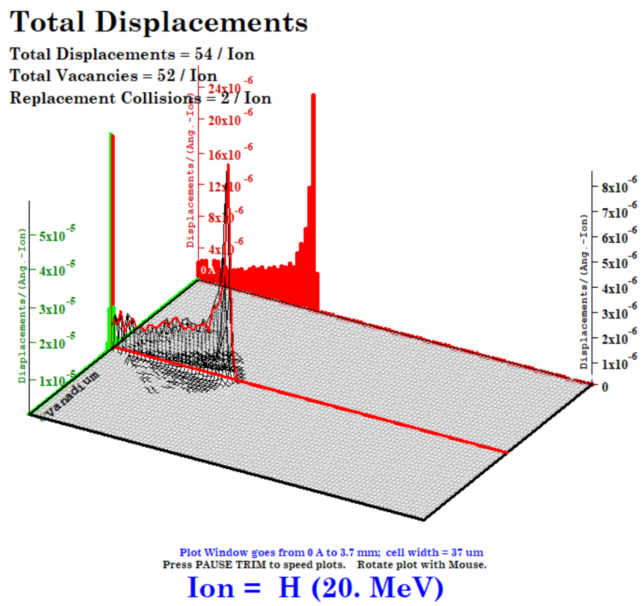

Figure 4.5 Depth and lateral radiation-damage distribution for 20 MeV proton irradiation of vanadium.

The plot illustrates where displacement production is spatially concentrated within the target and helps identify the local region relevant for peak-damage considerations shown in figure 4.5.

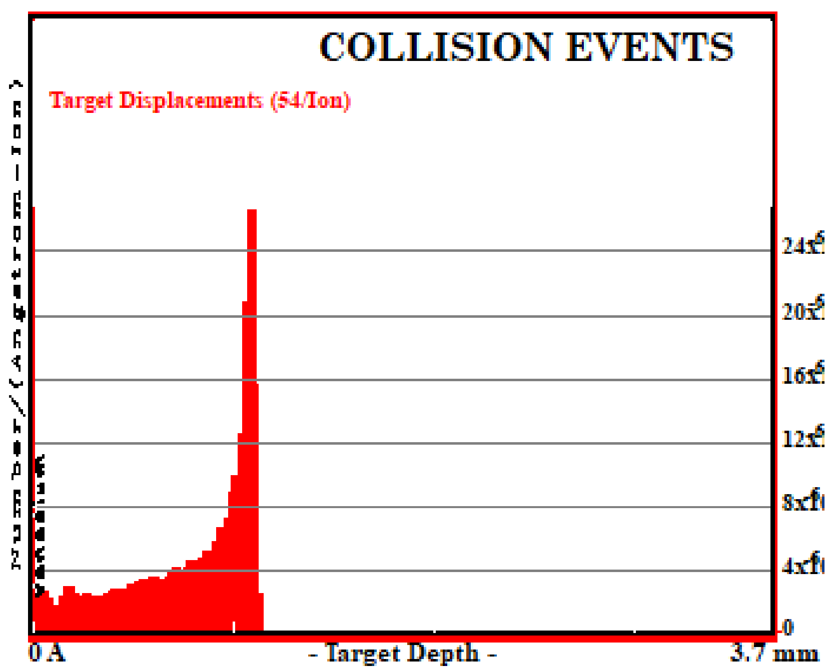

Figure 4.6 SRIM/TRIM target-displacement output for 20 MeV proton irradiation of vanadium.

The target-displacement yield extracted from this output shown in figure 4.6 is the displacement-related quantity used in the damage-rate calculation.

4.6.1 Annual Damage Accumulation in dpa/FPY

The annual damage accumulation was obtained by multiplying the damage rate in dpa s^{-1} by the number of seconds in one full power year. This converts the SRIM/TRIM-based damage rate into an operational quantity. The calculated range of 5.76–10.76 dpa/FPY indicates that vanadium experiences substantial displacement exposure during continuous 20 MeV proton operation. These values should be interpreted as NRT-dpa exposure values, not as direct stable-defect concentrations.

Using a first-order engineering damage threshold of 30 dpa, the estimated vanadium service life is approximately 2.79–5.21 years. The lower E_d case produces the shortest lifetime because it gives the highest calculated damage rate, whereas the upper E_d case gives the longest lifetime. The average E_d case gives a representative service-life estimate of approximately 4.09 years. This estimate does not define an exact failure time; rather, it indicates when accumulated damage may approach a level where irradiation-induced mechanical-property changes should be evaluated carefully.

Table 4.3 Estimated vanadium lifetime using average damage values averaged over the target depth and a 30 dpa first-order damage threshold.

Vanadium case	dpa/FPY	Lifetime to 30 dpa threshold
46 eV	10.76	3.27 years
57 eV	7.33	4.09 years
68 eV	5.76	5.21 years

4.7 Copper 3 MeV Proton Irradiation

4.8 SRIM Simulation Outputs

The copper simulations were performed for incident protons with an initial energy of 3 MeV using the same SRIM/TRIM workflow as for vanadium. Because the proton energy is lower, the penetration depth and the displacement distribution are shallower than in the 20 MeV vanadium case. The copper results are therefore interpreted as a near-surface irradiation case. This is relevant because near-surface damage can increase the importance of surface degradation, blistering, cracking, delamination and hydrogen-related effects, depending on the actual target design.

The copper output files include ion-distribution, recoil-statistics, energy-loss and target-displacement outputs. The main quantity used for the damage calculation is again the target-displacement yield per incident proton. The interpretation of copper damage requires caution because mechanical degradation is not determined by dpa alone. Published copper studies show that irradiation hardening, hydrogen accumulation and loss of ductility may become relevant at comparatively low damage levels, especially in near-surface regions [43–46].

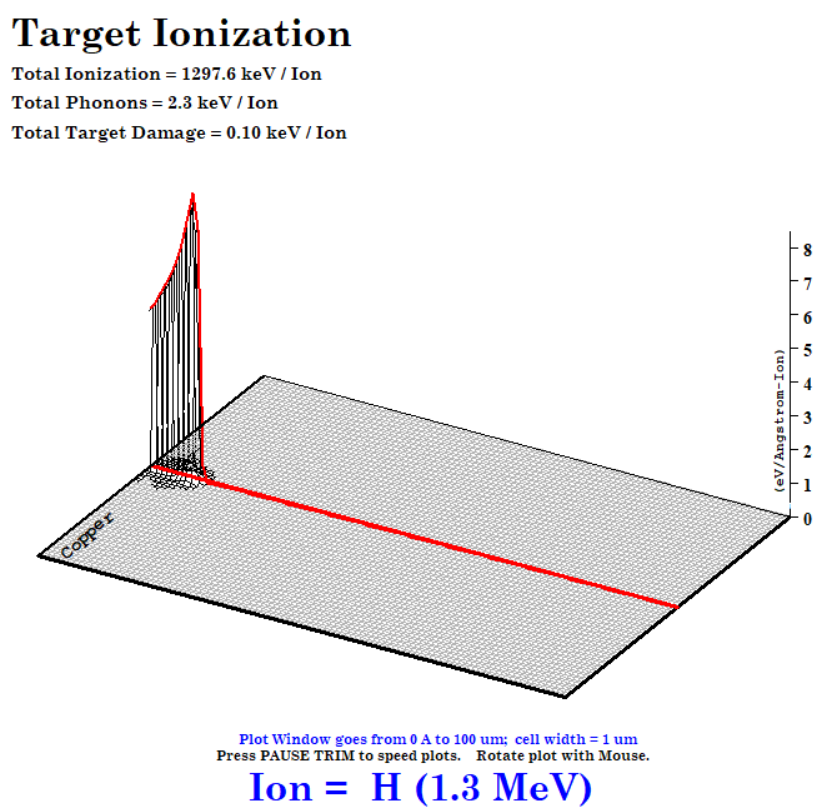

Figure 4.7 SRIM/TRIM output for 3 MeV proton irradiation of copper

The lower incident proton energy produces a shallower proton range and a correspondingly near-surface region of displacement production.

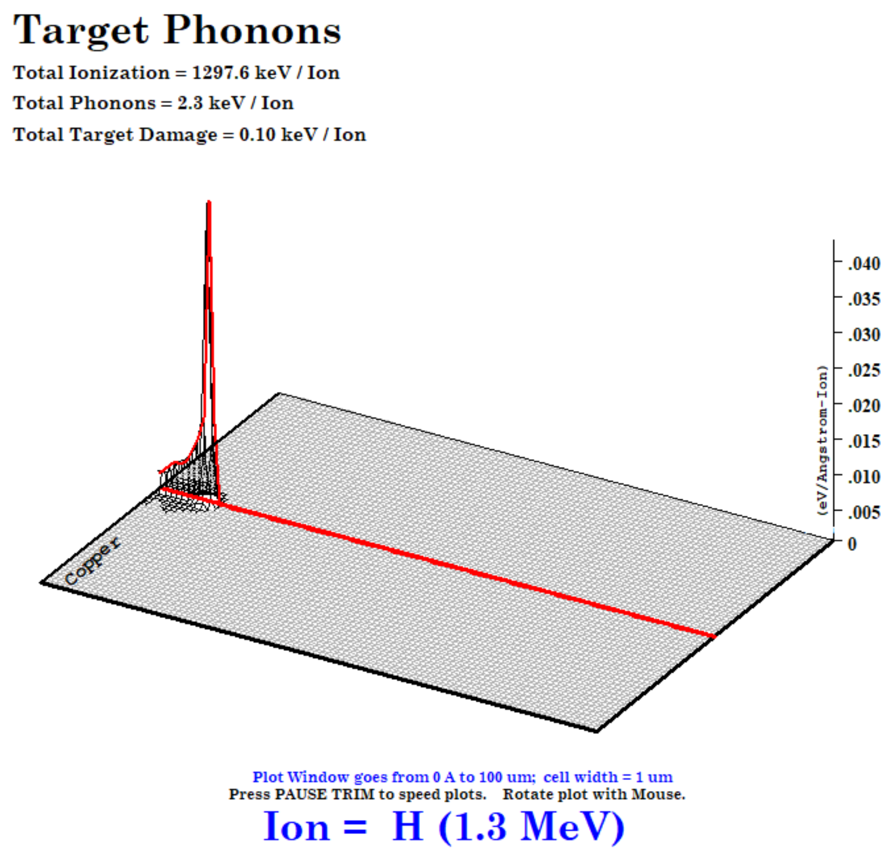

Figure 4.8 Copper 3 MeV simulation output showing depth-dependent ion or damage behavior.

The figure 4.8 supports the interpretation that the relevant displacement field is concentrated closer to the surface than in the 20 MeV vanadium case.

4.9 Proton Range and Near-Surface Damage

The range of 3 MeV protons in copper is much smaller than the range of 20 MeV protons in vanadium. This produces a shallow proton stopping region and a near-surface damage distribution in copper. In practical target components, such localization can increase the importance of local material degradation even when the total irradiated volume is smaller.

Because the copper damage profile is close to the surface, the local effect of beam loading may also become more critical. A shallow damaged layer can lead to a higher local displacement density for a given incident flux than a case where the damage is distributed through a deeper volume. This does not mean that copper must fail immediately, but it indicates that the local damage region, surface condition and cooling design must be considered together.

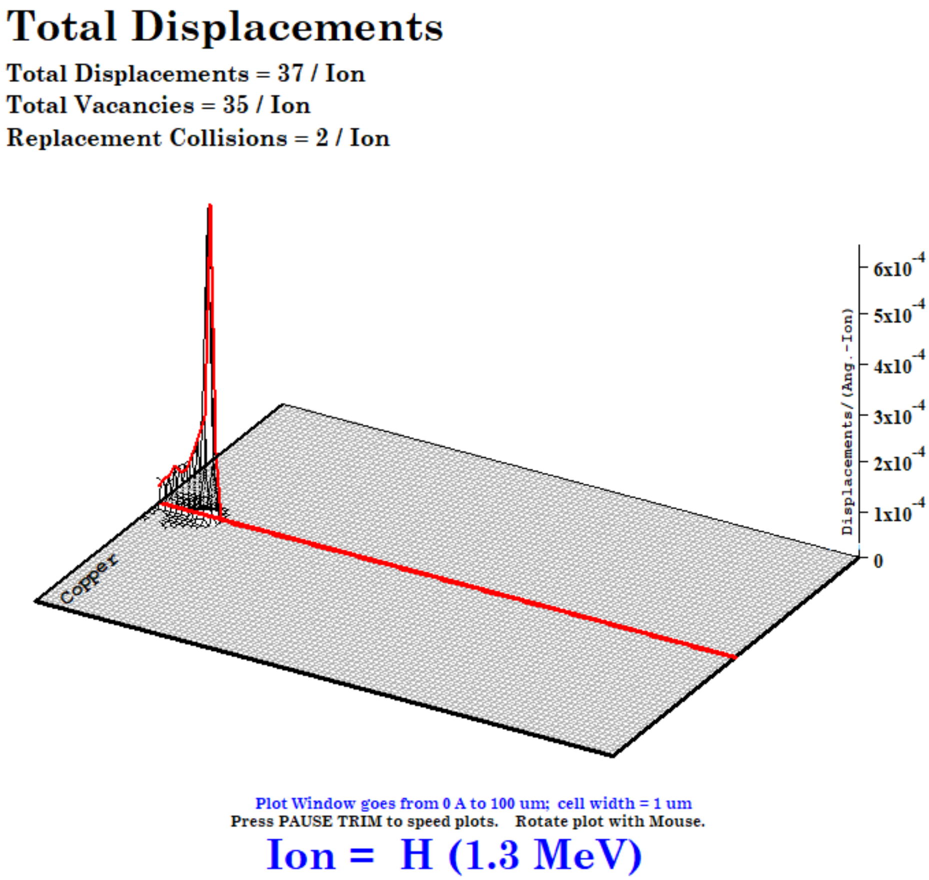

Figure 4.9 Copper 3 MeV SRIM/TRIM damage-related output.

The figure 4.9 indicates a shallow distribution of ion-induced effects and supports the interpretation of local near-surface displacement accumulation.

4.10 Displacement Yield for Lower, Average, and Upper E_d

For copper, the evaluated average threshold displacement energy is 30 eV with an uncertainty of approximately ±6 eV [42]. Therefore, three copper cases were evaluated: 24 eV, 30 eV and 36 eV. The average E_d case is treated as the representative calculation, while the lower and upper E_d cases define the uncertainty range. A lower E_d increases the probability that recoil events generate atomic displacements; it does not imply direct formation of macroscopic dislocations from every recoil event.

As in the vanadium case, the lower E_d case produces the largest calculated displacement yield, while the upper E_d case produces the smallest calculated displacement yield. The sensitivity range is important because copper has a lower average E_d than vanadium and therefore recoil events more readily exceed the displacement threshold. The values are interpreted as uncertainty cases in the SRIM/TRIM model rather than as design options.

Table 4.4 Threshold displacement energy cases used for the 3 MeV copper simulations.

Copper case	Threshold displacement energy E_d	Relative displacement expectation	Interpretation
Lower evaluated E_d	24 eV	Highest	Conservative high-damage case
Average E_d	30 eV	Reference	Representative case
Upper E_d	36 eV	Lowest	Lower-damage sensitivity case

4.10.1 Damage Rate Calculations

For copper, the same damage-rate equation was used, but with copper-specific material properties and beam parameters. Copper has a density of approximately 8.96 g cm^{-3} and a molar mass of 63.55 g mol^{-1}, giving an atomic number density of approximately 8.49×10^{22} atoms cm^{-3}. The SRIM/TRIM displacement yield was combined with the proton flux and the relevant averaging depth to calculate the annual NRT-dpa exposure.

The calculated annual damage accumulation for the copper 3 MeV case is approximately 28.23–47.63 dpa/FPY. The average E_d case gives approximately 36.03 dpa/FPY. These values indicate rapid accumulation of primary displacement exposure in the near-surface region. The engineering significance of this result must be interpreted using copper-specific damage-tolerance thresholds rather than by comparing the number directly with vanadium.

Table 4.5 Calculated annual damage accumulation for 3 MeV proton irradiation of copper

Copper E_d case	Calculated annual damage	Relative severity	Use in assessment
24 eV	47.63 dpa/FPY	Highest	Conservative high-damage case
30 eV	36.03 dpa/FPY	Reference	Main reported case
36 eV	28.23 dpa/FPY	Lowest	Upper-threshold sensitivity case

4.10.2 Near-Surface Damage Concentration

The near-surface concentration of displacement damage is a key feature of the copper result. For copper, local surface and subsurface damage may be relevant for deformation, blister formation, crack initiation and delamination, especially if stopped protons or transmutation products contribute to the local hydrogen inventory. Therefore, the dpa value alone is not sufficient to describe the operational risk; the depth location of the damage also matters.

The copper results should therefore be interpreted together with material-specific mitigation strategies. Increasing the assumed E_d in the simulation reduces the calculated damage only within the model uncertainty; it is not a technical method for reducing real damage. Practical mitigation would require measures such as optimized beam spreading, cooling design, surface management, reduced local flux or regular component replacement depending on the role of copper in the target assembly.

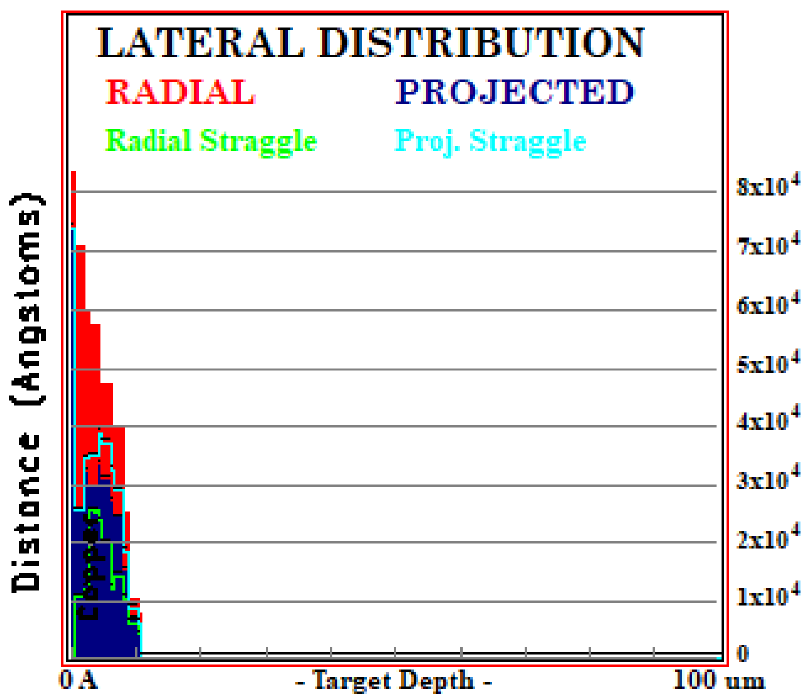

Figure 4.10 Additional copper 3 MeV SRIM/TRIM output used to interpret local displacement behavior and near-surface damage concentration.

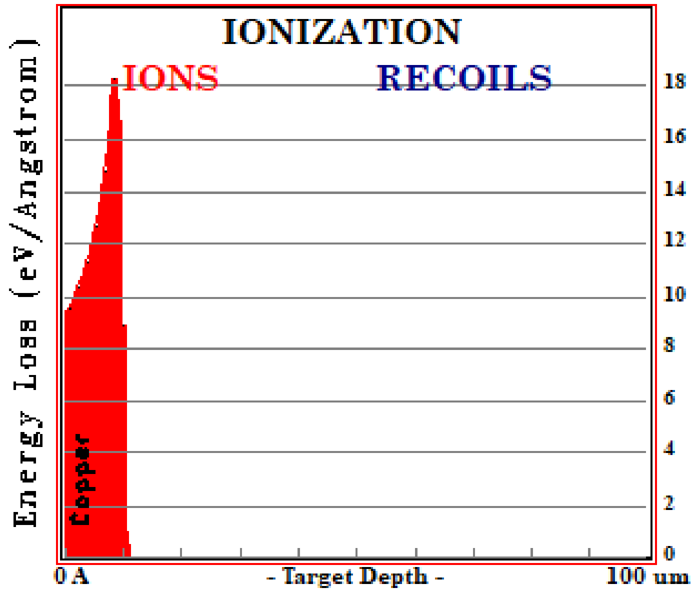

Figure 4.11 Copper 3 MeV simulation output showing depth-dependent behavior relevant to proton stopping and near-surface damage localization.

4.11 Annual Damage Accumulation in dpa/FPY

The annual damage-accumulation values indicate that copper may reach high NRT-dpa exposure within a relatively short operating period under the assumed 3 MeV irradiation condition. For a first-order service-life estimate, a conservative engineering screening threshold of 5 dpa was applied. This value should not be interpreted as a universal failure threshold for copper. Instead, it is used as a cautious assessment limit based on reported irradiation hardening, ductility degradation, and hydrogen-related damage mechanisms in copper. Using this threshold, the calculated service-life range is approximately 38–65 days, depending on the selected E_d value. The result therefore indicates that copper requires careful operational planning, monitoring, and possible replacement strategy when used as a lithium-target backing or support material under 3 MeV proton irradiation.

This calculation does not imply that copper will fail exactly at the calculated time in every design. Actual degradation depends on temperature, stress state, cooling design, beam distribution, hydrogen inventory, alloy condition, surface condition and the selected failure criterion. The calculation is therefore used as a warning indicator that copper exposed directly to the assumed 3 MeV proton beam would require careful design control and likely replacement planning.

Table 4.6 Estimated copper lifetime using a 5 dpa first-order damage threshold.

Copper case	dpa/FPY	Lifetime to 5 dpa threshold
24 eV	47.63	0.105 years ≈ 38 days
30 eV	36.03	0.139 years ≈ 51 days
36 eV	28.23	0.177 years ≈ 65 days

4.12 Separate Damage Assessment of the Two Target Cases

The vanadium and copper results are summarized together only to show how the same SRIM/TRIM-based methodology behaves when applied to two different irradiation cases. They should not be interpreted as a direct material competition for the same target. Vanadium is assessed for the 20 MeV target case and copper is assessed for the 3 MeV target/backing or diagnostic case. The calculated annual damage ranges are 5.76–10.76 dpa/FPY for vanadium and 28.23–47.63 dpa/FPY for copper.

The difference between the two result sets arises from the combined effects of incident proton energy, stopping behavior, material density, atomic number density, threshold displacement energy and damage localization. Vanadium has a higher evaluated E_d, while copper has a lower evaluated E_d and a shallower near-surface damage profile in the investigated 3 MeV case. For this reason, each material must be assessed using its own target function and material-specific damage tolerance.

Table 4.7 Separate summary of vanadium and copper damage results for their respective target cases.

Parameter	Vanadium 20 MeV	Copper 3 MeV	Implication
E_d range	46–68 eV	24–36 eV	Lower evaluated E_d gives higher displacement probability
Average dpa/FPY	7.33	36.03	Higher calculated dpa/FPY in 3 MeV copper case
Damage profile	Deeper distributed region	Near-surface concentration	3 MeV copper case has near-surface concentration
First-order lifetime	≈4.09 years at average E_d	≈51 days at average E_d	Different service-life estimates for different target cases
Main risk	Long-term hardening and dose accumulation	Hydrogen blistering and ductility loss	Different mitigation strategies required

4.13 Threshold Displacement Energy Sensitivity

The threshold-displacement-energy sensitivity study shows that the calculated dpa rates for both materials are strongly influenced by uncertainty in E_d. In both cases, lower E_d values produce higher calculated dpa/FPY because recoil events are more likely to exceed the displacement threshold. Upper E_d values produce lower calculated dpa/FPY because fewer recoil events satisfy the displacement criterion.

For vanadium, the calculated annual damage accumulation ranges from 5.76 to 10.76 dpa/FPY. For copper, the corresponding range is 28.23 to 47.63 dpa/FPY. These ranges should be interpreted as model uncertainty caused by the selected E_d values. The average E_d cases, 57 eV for vanadium and 30 eV for copper, are used as the main representative values in the service-life discussion.

Table 4.8 Threshold displacement energy sensitivity comparison.

Material	Lowest dpa/FPY	Average dpa/FPY	Highest dpa/FPY	Conclusion
Vanadium	5.76	7.33	10.76	Multi-year first-order service-life estimate
Copper	28.23	36.03	47.63	Requires mitigation or planned replacement

4.14 Lifetime Estimation Results

Service-life estimation was carried out by dividing the selected first-order damage threshold by the calculated annual damage accumulation. A 30 dpa threshold was used for the vanadium assessment because literature on V–Cr–Ti alloys reports retained ductility at high accumulated damage. A 5 dpa threshold was used for the copper assessment as a conservative first-order limit reflecting the more severe hardening and hydrogen-related degradation reported for copper systems. These thresholds are engineering assumptions for comparative assessment, not universal failure limits.

Using these assumptions, the estimated vanadium service life is approximately 2.79–5.21 years, while the copper service-life estimate is approximately 38–65 days. These values indicate when accumulated NRT-dpa exposure reaches the selected threshold; they do not predict an exact mechanical failure time. The results are intended to guide whether a target concept may be suitable for continuous operation, whether mitigation is required, or whether regular replacement must be planned.

Table 4.9 First-order lifetime estimation for vanadium and copper.

Material	Damage threshold used	dpa/FPY range	Estimated lifetime range	Operational interpretation
Vanadium	30 dpa	5.76–10.76	2.79–5.21 years	Candidate for 20 MeV target assessment
Copper	5 dpa	28.23–47.63	38–65 days	Requires protected, replaceable or mitigated role

4.15 Peak Damage-Rate Assessment for Minimum E_d

The peak damage-rate assessment was added to identify the most severe local irradiation condition in the target material. In contrast to the average damage values, the peak value corresponds to the region where SRIM/TRIM predicts the maximum local displacement production. This value is useful for estimating the lower-bound service life of the most highly damaged target region.

The peak damage rate was calculated from the SRIM displacement output using the following relation adopted from the SRIM-based methodology:

$$R_{peak} = (n_{disp,peak} \cdot \varphi) / (d \cdot N_{atom}) \quad (4.1)$$

As shown in Eq. 4.1 R_{peak} is the peak damage rate in dpa s^{-1}, $n_{disp,peak}$ is the peak target displacement yield obtained from SRIM, φ is the proton flux, d is the target thickness or averaging depth, and N_{atom} is the atomic number density.

The annual peak damage accumulation was calculated as:

$$\text{dpa/FPY} = R_{peak} \cdot t_{FPY} \quad (4.2)$$

$$t_{FPY} = 365 \times 24 \times 3600 = 3.1536 \times 10^7 \text{ s}$$

The corresponding service life was then estimated from:

$$t_{life} = \text{dpa}_{\text{limit}} / (\text{dpa/FPY}) \quad (4.3)$$

Table 4.10 Peak damage-rate assessment using minimum Ed values.

Material	Minimum E_d (eV)	R_{peak} (dpa s^{-1})	Peak damage (dpa/FPY)	Estimated service life
Vanadium	46	1.60 × 10−6	50.5	0.6 year
Copper	24	7.51 × 10−5	2369.9	7.7 days

The values in Table 4.10 represent conservative local peak-damage estimates based on the minimum E_d cases. For vanadium, the peak damage rate was calculated as 1.60×10^{-6} dpa s^{-1}, which corresponds to 50.5 dpa/FPY and an estimated service life of approximately 0.6 year. For copper, the peak damage rate consistent with 2369.9 dpa/FPY is 7.51×10^{-5} dpa s^{-1}, giving an estimated service life of approximately 7.7 days. These peak values are not average target damage values. Instead, they identify the most radiation-sensitive region of the target and can be used in the conclusion as a conservative lower-bound service-life estimate.

4.16 Summary of Results

The SRIM/TRIM simulations indicate that vanadium under 20 MeV proton irradiation accumulates substantial but manageable primary displacement exposure under the assumptions used in this thesis. The calculated annual damage range is 5.76–10.76 dpa/FPY, with 7.33 dpa/FPY as the representative average E_d case. When a first-order 30 dpa threshold is applied, the resulting service-life estimate lies in the multi-year range.

For copper under 3 MeV proton irradiation, the calculated annual damage accumulation is 28.23–47.63 dpa/FPY, with 36.03 dpa/FPY as the representative average E_d case. Using a conservative 5 dpa first-order threshold gives a service-life estimate of 38–65 days. This result indicates that copper exposed directly to the assumed 3 MeV proton field would require mitigation strategies, design control or planned replacement depending on its function in the target assembly.

The main conclusion of Chapter 4 is that both materials must be assessed within their own target context. Vanadium shows a multi-year first-order service-life estimate for the 20 MeV case, whereas copper shows a much shorter first-order service-life estimate for the 3 MeV case. These results form the basis for the discussion of material response, hydrogen effects, design implications and methodological limitations in Chapter 5.

5 Discussion

This chapter discusses the calculated results in the context of radiation-damage methodology, SRIM/TRIM uncertainty, material response and target sustainability for HBS-related applications. The discussion emphasizes that vanadium and copper are not treated as interchangeable materials for the same target. Instead, vanadium is evaluated for the 20 MeV target case, while copper is evaluated for the 3 MeV target/backing or diagnostic case.

5.1 arc-dpa Methodology and Limitations

The primary damage quantity reported in this thesis is NRT-dpa because the calculation is based on SRIM/TRIM displacement outputs and because NRT-dpa is widely used as an exposure parameter for comparing irradiation conditions [37–40]. In this context, dpa is not interpreted as the actual concentration of stable defects. It is used as a standardized measure of primary displacement exposure.

The arc-dpa model was developed to account for athermal recombination during displacement cascades [41,49]. In energetic cascades, many initially displaced atoms recombine before becoming stable defects. Therefore, NRT-dpa tends to overestimate stable defect production and should not be treated as a microstructural state variable. The arc-dpa model reduces the NRT estimate by applying a defect-production efficiency factor.

For the present thesis, reporting NRT-dpa is methodologically appropriate because the objective is to provide a first-order exposure and service-life assessment rather than an exact prediction of surviving defect inventory. The use of the same NRT-based workflow for both target cases ensure methodological consistency. However, future work using arc-dpa or molecular dynamics would provide a more refined estimate of stable defect production.

Table 5.1 Methodological comparison of NRT-dpa and arc-dpa in this thesis.

Issue	NRT-dpa implication	arc-dpa implication
Defect recombination	Not fully corrected	Partly corrected through efficiency factor
Use in this thesis	Main reported quantity	Discussed as future refinement
Comparability	High across literature	More material-specific
Limitation	Overestimates surviving defects	Needs reliable correction parameters

5.2 SRIM/TRIM Validation and Uncertainties

SRIM/TRIM is widely used for ion-irradiation studies because it provides useful estimates of ion range, stopping behavior, recoil production and displacement exposure [37,38]. Its main advantage is that it offers a reproducible and practical workflow for comparing different irradiation scenarios. In this thesis, SRIM/TRIM is used as a primary-damage tool rather than as a complete microstructural evolution model.

The main limitation of SRIM/TRIM is its reliance on the binary-collision approximation. In this approximation, cascades are represented as sequences of individual collisions, while many-body thermal-spike behavior and long-time defect evolution are not fully described. Therefore, SRIM/TRIM results should be interpreted as estimates of primary displacement exposure rather than direct predictions of final material microstructure.

Several sources of uncertainty affect the calculated dpa rates. The first is the threshold displacement energy E_d, which was addressed by using lower, average and upper cases. The second is the selected damage-averaging depth, because average and peak damage values can differ significantly. Additional uncertainty arises from the assumed beam profile, idealized target geometry, material purity and the absence of coupled thermal-mechanical analysis.

Because vanadium and copper correspond to different target cases, the results are not used as a direct replacement comparison. Instead, the uncertainty analysis shows whether each material remains within an acceptable first-order service-life range for its own irradiation scenario. For copper, the shallow damage profile and high annual dpa/FPY indicate that local mitigation and replacement planning are important design considerations.

Table 5.2 Main uncertainty sources in SRIM/TRIM-based damage assessment.

Uncertainty source	Effect on results	Treatment in thesis
Threshold displacement energy	Changes displacement yield and dpa/FPY	Lower, average and upper cases used
Damage averaging depth	Changes average versus peak damage rate	Depth-resolved profiles discussed
SRIM BCA approximation	Limits detailed cascade physics	Results interpreted as primary damage estimates
Beam profile	Affects local flux and peak damage	Uniform-area assumption used
Temperature effects	Affects diffusion and recombination	Discussed as limitation

5.3 Comparison with Tantalum HBS Reference

The HBS-related study by Ophoven et al. provides an important methodological reference because it demonstrates how Monte Carlo outputs can be converted into average and peak dpa rates for an irradiated neutron-emitting target [50]. The relevance of that work for the present thesis is methodological: it shows how simulation output, beam parameters and target properties can be combined to estimate annual displacement exposure.

The tantalum reference case is not used as a direct numerical benchmark for vanadium or copper because the material, proton energy, geometry and target function differ. However, the underlying methodology is comparable. Ophoven et al. showed that radiation damage can be spatially non-uniform and that both average and local peak damage values are important for lifetime assessment [50].

A similar methodological observation applies to the present HBS candidate materials. The vanadium 20 MeV case produces a deeper and more spatially distributed damage profile, whereas the copper 3 MeV case produces a shallower near-surface damage profile. These differences do not by themselves determine whether a material is acceptable; they define which region of each target requires the greatest design attention.

Table 5.3 Methodological comparison with the tantalum HBS reference study.

Aspect	Tantalum HBS reference	Present thesis
Material	Tantalum	Vanadium and copper
Proton energy	70 MeV	20 MeV and 3 MeV
Main method	Monte Carlo dpa calculation	SRIM/TRIM NRT-dpa calculation
Main output	Average and peak damage rates	dpa/FPY and lifetime estimates
Shared relevance	Target lifetime assessment	Target sustainability comparison

5.4 Vanadium Sustainability Assessment

The vanadium results indicate substantial displacement exposure during continuous operation under 20 MeV proton irradiation. However, the calculated damage rate is compatible with a multi-year first-order service-life estimate when the 30 dpa threshold used in this thesis is applied. The average E_d case gives approximately 7.33 dpa/FPY and a representative lifetime of approximately 4.09 years.

The literature on V–Cr–Ti alloys supports this assessment because these alloys have been investigated for irradiation environments and can retain ductility at high accumulated damage levels [47,48]. The relevance of this literature is not that vanadium is automatically qualified for HBS, but that the calculated dpa levels fall within a range where mechanical-property data suggest that useful ductility may still be retained, depending on temperature, alloy condition and stress state.

The assessment of vanadium is further supported by its hydrogen-related properties. Vanadium has temperature-dependent hydrogen permeability, which can support hydrogen removal during operation. First-principles studies indicate that significant vacancy stabilization and high hydrogen concentrations are required for substantial hydrogen-bubble formation in vanadium. These properties reduce, but do not eliminate, the need for hydrogen management in the final target design.

The main design implication is that vanadium should be evaluated not only as pure vanadium but also as V–4Cr–4Ti or a similar optimized alloy. Chromium and titanium additions can influence oxygen control, mechanical behavior and irradiation response. However, the exact alloy condition, manufacturing route and impurity level must be defined before a final qualification decision can be made.

Table 5.4 Main reasons for the favorable vanadium sustainability assessment.

Vanadium advantage	Reason for relevance
Higher evaluated E_d	Reduces calculated displacement production for a given damage-energy transfer
Distributed damage profile	Distributes damage over a deeper region in the 20 MeV case
Ductility retention reported in literature	Supports use of higher damage threshold
Favorable hydrogen-related behavior	Supports hydrogen management, subject to operating temperature
V–4Cr–4Ti alloy option	Provides an advanced radiation-resistant candidate

5.5 Copper Sustainability Assessment

The copper results indicate a limited first-order service-life estimate for direct exposure to the assumed 3 MeV proton irradiation conditions. The average E_d case gives approximately 36.03 dpa/FPY, and the assumed 5 dpa first-order threshold is reached after approximately 51 days. This result should be interpreted within the 3 MeV copper target/backing or diagnostic context, not as a direct competition with the vanadium 20 MeV target case.

The high calculated damage rate means that copper would require careful planning of mitigation and replacement if it is directly exposed to the proton beam. Copper is also known to be prone to strong irradiation hardening because irradiation-induced defects impede dislocation motion [45,46]. This hardening can reduce plastic deformation capacity and increase sensitivity to cracking or fracture under thermal-mechanical loading.

Hydrogen-related degradation is an additional concern for copper. Proton irradiation is not identical to hydrogen implantation; however, stopped protons and transmutation products can contribute to a local hydrogen inventory. Literature reports show that copper can be prone to hydrogen blistering and early ductility degradation under hydrogen-containing irradiation conditions [43,44]. This is particularly relevant when the damage distribution is concentrated near the surface.

Under these assumptions, copper should not be considered a long-life directly irradiated component without mitigation. It may still be useful as a backing material, heat sink, sacrificial layer or replaceable component if the design limits the accumulated damage, controls the local thermal load and includes a realistic replacement strategy.

Table 5.5 Main reasons for the limited copper sustainability assessment.

Copper limitation	**Consequence for target use**
Lower evaluated Ed	Higher calculated displacement production
Near-surface damage concentration	May increase risk of near-surface degradation
Strong irradiation hardening	Reduced plastic deformation capacity
Hydrogen blistering	Surface degradation and possible delamination
Short lifetime estimate	Replacement or mitigation required

5.6 Mechanical Property Implications

The calculated dpa values must be interpreted in terms of mechanical-property changes. In general, irradiation-induced defects impede dislocation motion, which increases yield strength and hardness. This irradiation hardening can be useful up to a point, but excessive hardening often reduces ductility and fracture tolerance.

Young’s modulus alone is not a reliable indicator of target sustainability. Both vanadium and copper may retain relatively stable elastic stiffness under irradiation, while their ductility and fracture behavior can evolve very differently. Therefore, service-life assessment must consider hardness, yield strength, uniform elongation, fracture morphology, swelling and hydrogen-related degradation together.

For vanadium, the calculated damage accumulation can be compared with literature data showing retained elongation and ductile fracture behavior in V–Cr–Ti alloys at high damage levels [47,48]. This supports the use of a higher first-order damage threshold for vanadium in the present assessment. For copper, the calculated annual damage is high relative to its assumed 5 dpa threshold, and literature reports of hardening and ductility degradation indicate that direct exposure would require mitigation or frequent replacement.

Table 5.6 Mechanical-property implications of calculated radiation damage.

Property	Vanadium implication	Copper implication
Young's modulus	Likely relatively stable	Likely relatively stable but not sufficient
Yield strength / hardness	Predictable hardening	Strong hardening, possible embrittlement
Uniform elongation	Retention reported at high dose	Can collapse with hydrogen
Fracture mode	Ductile behavior can remain	Intergranular or brittle behavior possible
Design consequence	Longer target lifetime possible	Replacement strategy required

5.7 Hydrogen, Blistering, and Embrittlement Implications

Hydrogen-related effects are important for both target cases, but the mechanisms must be described carefully. Proton irradiation can increase the hydrogen inventory if protons stop in the material or if nuclear reactions generate hydrogen isotopes. The presence of hydrogen can interact with vacancies, dislocations, grain boundaries and surfaces, which may contribute to embrittlement, bubble formation or blistering.

For vanadium, hydrogen can diffuse relatively effectively at elevated temperature, which may reduce local hydrogen accumulation. In addition, first-principles calculations indicate that significant vacancy stabilization and high hydrogen concentration are required before substantial hydrogen-bubble formation becomes favorable in the bulk material. This makes hydrogen management more feasible for vanadium, but it remains an essential design requirement.

For copper, hydrogen-related degradation is more challenging. Literature reports indicate hydrogen blistering and loss of plasticity in copper under hydrogen-containing irradiation conditions [43,44]. In the 3 MeV case, both displacement damage and potential hydrogen accumulation are concentrated closer to the surface, which may increase the risk of blistering, near-surface cracking or delamination.

The practical implication is that hydrogen management must be included in target design. For vanadium, temperature-controlled operation may assist hydrogen removal. For copper, direct exposure should be minimized where possible, and mitigation strategies such as surface protection, reduced local flux, beam spreading or planned replacement may be required.

Table 5.7 Hydrogen-related implications for vanadium and copper target use.

Hydrogen-related factor	Vanadium	Copper
Hydrogen permeability	Favorable and temperature dependent	Less favorable for safe removal
Bubble nucleation	High barrier reported	More susceptible at defects/surfaces
Blistering risk	Temperature dependent, manageable with conditions	Important concern under hydrogen-containing irradiation
Operational implication	Temperature optimization important	Direct exposure should be minimized

5.8 Operational and Sustainability Implications

The results provide guidance for the two HBS-related target cases studied here. Vanadium is evaluated as a candidate for the 20 MeV proton-irradiated target case and shows a multi-year first-order service-life estimate under the assumptions used. This assessment is supported by literature reporting favorable ductility retention and hydrogen behavior in vanadium-based alloys.

Copper is evaluated for the 3 MeV target/backing or diagnostic case. The calculated annual damage accumulation is high and concentrated near the surface. Therefore, copper exposed directly to this proton field should be treated as a limited-life component unless mitigation strategies are implemented. It may still be suitable in protected, cooled, replaceable or backing roles depending on the final target design.

Maintenance and replacement cycles must therefore be included in the sustainability assessment. A material with a multi-year first-order service-life estimate can support a stable operational strategy, whereas a material with a weeks-to-months estimate requires planned replacement, reduced exposure or design mitigation.

Table 5.8 Operational implications of the sustainability assessment.

Design issue	Vanadium strategy	Copper strategy
Direct proton exposure	Candidate for evaluation with monitoring	Minimize or mitigate if directly exposed
Cooling design	Optimize around damage peak depth	Control near-surface heat and hydrogen effects
Replacement interval	Multi-year first-order estimate	Weeks-to-month's estimate
Recommended role	20 MeV target candidate	Backing, heat sink, sacrificial or replaceable component
Future validation	20 MeV irradiation test required	Hydrogen blistering and replacement tests required

5.9 Limitations of the Present Work

The present work demonstrates the usefulness of a first-order computational sustainability analysis, but it does not experimentally validate the target materials. Several limitations must therefore be acknowledged. First, SRIM/TRIM calculates primary displacement exposure, while long-term microstructural evolution, defect migration, thermal recovery and stress-assisted damage are not explicitly modelled.

Second, secondary neutron damage is not explicitly calculated in the present SRIM/TRIM framework. A full qualification study would require coupled particle-transport, thermal-mechanical and radiation-damage analysis. Such modelling would provide a more precise estimate of target performance under actual HBS operating conditions.

Third, the calculations are based on idealized beam and material assumptions. The local damage field may be modified by the real beam profile, target geometry, cooling channels, surface roughness, material purity and manufacturing history. Therefore, the calculated service lives should be treated as first-order engineering estimates rather than final qualification values.

Despite these limitations, the study provides a consistent and reproducible assessment of two independent HBS-related irradiation cases. The results indicate that vanadium has a multi-year first-order service-life estimate for the 20 MeV target case, while copper would require mitigation or regular replacement in the 3 MeV case if directly exposed to the proton beam.

5.10 Summary of Discussion

The discussion shows that the calculated results are physically consistent with established radiation-damage theory and with the material-response literature. Vanadium has a higher evaluated E_d, a deeper damage profile and literature support for ductility retention in V–Cr–Ti alloys. Copper has a lower evaluated E_d, a shallow near-surface damage profile and literature evidence for irradiation hardening and hydrogen-related degradation.

NRT-dpa is suitable as a standardized primary-damage exposure metric, but it should not be interpreted as final defect concentration. Future improvement would require arc-dpa correction, molecular dynamics support, experimental irradiation data and coupled thermal-mechanical modelling. These additions would improve the precision of the service-life estimate and support full material qualification.

6 Conclusion and Outlook

This thesis addressed proton induced radiation damage and the viability of vanadium and copper target materials for HiCANS (high current driven neutron source) applications. The interaction of protons with target materials was simulated using SRIM/TRIM Monte Carlo simulations, and the results quantified to estimate the amount of displacement damage, and the operational lifetime, of the investigated targets. The study was based on the following two irradiation conditions: 20 MeV proton irradiation for vanadium and 3 MeV proton irradiation for copper, which are relevant to the High Brilliance neutron Source (HBS) project.

In the simulations, the proton penetration, energy deposition and formation of displacements were calculated in the target materials. In order to obtain the target displacement values, a damage rate was calculated by adopting NRT-dpa approach based on proton flux, atomic number density and irradiation conditions. Lower, mean and upper threshold displacement energies E_d were determined to account for uncertainties in the production of displacement. A realistic range of uncertainty was given by the lower and upper E_d values, and the mean E_d values gave the most probable service-life estimates. These results showed that the accumulation of radiation damage is strongly affected by proton energy, material property, and the assumptions of threshold displacement energy. Additionally, the calculated damage distributions allowed target service life to be estimated under continuous operation.

In addition to average damage-rate calculations, peak damage-rate values were evaluated to identify the most severely irradiated regions of each target. For the minimum E_d case, vanadium showed a peak damage rate of 1.60×10^{-6} dpa s^{-1}, corresponding to 50.5 dpa/FPY and an estimated conservative service life of approximately 0.6 year. Copper showed a peak damage rate of 7.51×10^{-5} dpa s^{-1}, corresponding to 2369.9 dpa/FPY and an estimated service life of approximately 7.7 days. These peak values represent conservative lower-bound service-life estimates and identify the most radiation-sensitive regions of the targets.

Using damage values averaged over the target depth, vanadium exhibited a damage accumulation rate of 10.76 dpa/FPY for the minimum E_d case, resulting in an estimated service life of 3.27 years for a 30 dpa threshold. The corresponding mean and upper E_d

cases yielded longer service-life estimates, demonstrating the sensitivity of lifetime predictions to the choice of threshold displacement energy. By evaluating lower, mean, and upper E_d values together, a realistic uncertainty range 0.6 - 5.21 years for vanadium target lifetime was established.

The method introduced in this study offers a viable approach and provides a reliable estimate of the operational target towards the study and simulation of radiation damage in accelerator target materials. However, the loss of displacement alone is not sufficient to fully consider the degradation of materials in operation. The inclusion of experimental irradiation data, temperature effects, hydrogen and helium accumulation, irradiation-enhanced diffusion and changes in mechanical properties caused by irradiation should be incorporated in future work. Other advanced damage models, including arc-dpa and molecular dynamics-based ones, might also be used to increase the capability for lifetime predictions. Those investigations could help to better understand target performance and also pave the way for design of reliable and sustainable target systems for future accelerator-driven neutron sources.

7 References

[1] Brückel, T., et al. (2023). Technical Design Report HBS, Volume 2. Forschungszentrum Jülich GmbH Zentralbibliothek.

[2] Ophoven, N., Mauerhofer, E., Li, J., Rücker, U., Zakalek, P., Baggemann, J., Gutberlet, T., Brückel, T. and Langer, C. (2021). Monte Carlo simulation of proton- and neutron-induced radiation damage in a tantalum target irradiated by 70 MeV protons. Applied Physics A, 127, 576. https://doi.org/10.1007/s00339-021-04713-4

[3] Nordlund, K., Sand, A.E., Granberg, F., Zinkle, S.J., Stoller, R., Averback, R.S., Suzudo, T., Malerba, L., Banhart, F., Weber, W.J., Willaime, F., Dudarev, S. and Simeone, D. (2015). Primary Radiation Damage in Materials. NEA/NSC/DOC(2015)9. OECD Nuclear Energy Agency.

[4] Konobeyev, A.Yu., Fischer, U., Korovin, Yu.A. and Simakov, S.P. (2017). Evaluation of effective threshold displacement energies and other data required for the calculation of advanced atomic displacement cross-sections. Nuclear Energy and Technology, 3(3), 169–175. https://doi.org/10.1016/j.nucet.2017.08.007

[5] Malo, S., Giroux, E., Araque Camacho, N., Chikada, T. and Tanaka, S. (2022). Experimental determination of hydrogen isotope transport parameters in vanadium. Membranes, 12(6), 579. https://doi.org/10.3390/membranes12060579

[6] Su, Z., Wang, S., Lu, C. and Peng, Q. (2020). Relationship between the behavior of hydrogen and hydrogen bubble nucleation in vanadium. Materials, 13(2), 322. https://doi.org/10.3390/ma13020322

[7] Kaletta, D. (1976). Helium-induced blistering in vanadium and vanadium-titanium alloys. Journal of Nuclear Materials, 63(3), 347–355.

[8] Cingoranelli, S.J., Putnam, E.E., Appiah, J.P., Rider, J., Burnett, L. and Lapi, S.E. (2024). Production of high purity 47Sc from proton irradiation of natural vanadium targets. EJNMMI Radiopharmacy and Chemistry, 9, 89. https://doi.org/10.1186/s41181-024-00321-8

[9] Chung, H.M., Loomis, B.A. and Smith, D.L. (1995). Properties of V–4Cr–4Ti for application as fusion reactor structural components. Fusion Engineering and Design, 29, 455–464. https://doi.org/10.1016/0920-3796(95)80053-Z

[10] Shen, J., Nagasaka, T., Tokitani, M., Muroga, T., Kasada, R. and Sakurai, S. (2022). Effects of titanium concentration on microstructure and mechanical properties of high-purity vanadium alloys. Materials & Design, 224, 111390. https://doi.org/10.1016/j.matdes.2022.111390

[11] Kazakov, V.A., Ostrovsky, Z., Goncharenko, Y. and Chakin, V. (2000). Features of radiation damage of vanadium and its alloys at a temperature of 330–340°C. Journal of Nuclear Materials, 283–287, 727–730. https://doi.org/10.1016/S0022-3115(00)00218-X

[12] Kiener, D., Hosemann, P., Maloy, S.A. and Minor, A.M. (2011). In situ nanocompression testing of irradiated copper. Nature Materials, 10(8), 608–613. https://doi.org/10.1038/nmat3055

[13] Barbe, V., Debelle, A. and Davydov, M. (2018). Hydrogen implantation and complete ductility loss in copper. arXiv preprint, 1803.03983.

[14] Serafim, C., Calatroni, S., Djurabekova, F., Peacock, R., et al. (2025). Effects of H− low beam irradiation and high field pulsing tests in different metals. Physical Review Accelerators and Beams, 28(1), 013101. https://doi.org/10.1103/PhysRevAccelBeams.28.013101

[15] Qadr, M.R. (2020). Effect of ion irradiation on the mechanical properties of high and low copper. Atom Indonesia, 46(2), 119–124. https://doi.org/10.17146/aij.2020.923

[16] Kinchin, G.H. and Pease, R.S. (1955) 'The displacement of atoms in solids by radiation', Reports on Progress in Physics, 18(1), pp. 1–51. doi:10.1088/0034-4885/18/1/301.

[17] Norgett, M.J., Robinson, M.T. and Torrens, I.M. (1975) 'A proposed method of calculating displacement dose rates', Nuclear Engineering and Design, 33(1), pp. 50–54. doi:10.1016/0029-5493(75)90035-7.

[18] Ziegler, J.F., Ziegler, M.D. and Biersack, J.P. (2010) 'SRIM – The stopping and range of ions in matter', Nuclear Instruments and Methods in Physics Research Section B, 268(11–12), pp. 1818–1823. doi:10.1016/j.nimb.2010.02.091.

[19] Stoller, R.E., Toloczko, M.B., Was, G.S., Certain, A.G., Dwaraknath, S. and Garner, F.A. (2013) 'On the use of SRIM for computing radiation damage exposure', Nuclear Instruments and Methods in Physics Research Section B, 310, pp. 75–80. doi:10.1016/j.nimb.2013.05.008.

[20] Nordlund, K., Djurabekova, F., Sand, A.E., Granberg, F., Zinkle, S.J., Stoller, R., Averback, R.S., et al. (2018) ‘Improving atomic displacement and replacement calculations with physically realistic damage models’, Nature Communications, 9, 1084. doi:10.1038/s41467-018-03415-5.

[21] OECD Nuclear Energy Agency (2015) Primary Radiation Damage in Materials: Review of Current Understanding and Proposed New Standard Displacement Damage Model to Incorporate Cascade Defect Production Efficiency and Mixing Effects. NEA/NSC/DOC(2015)9. Paris: OECD/NEA.

[22] Konobeyev, A.Yu., Fischer, U., Korovin, Yu.A. and Simakov, S.P. (2017) ‘Evaluation of effective threshold displacement energies and other data required for the calculation of advanced atomic displacement cross-sections’, Nuclear Energy and Technology, 3, pp. 169–175. doi:10.1016/j.nucet.2017.08.007.

[23] Ophoven, N., Mauerhofer, E., Li, J., Rücker, U., Zakalek, P., Baggemann, J., Gutberlet, T., Brückel, T. and Langer, C. (2021) ‘Monte Carlo simulation of proton- and neutron-induced radiation damage in a tantalum target irradiated by 70 MeV protons’, Applied Physics A, 127, 576. doi:10.1007/s00339-021-04713-4.

[24] Zinkle, S.J. and Busby, J.T. (2009) ‘Structural materials for fission & fusion energy’, Materials Today, 12(11), pp. 12–19. doi:10.1016/S1369-7021(09)70294-9.

[25] Was, G.S. (2017) Fundamentals of Radiation Materials Science: Metals and Alloys. 2nd edn. New York: Springer. doi:10.1007/978-1-4939-3438-6.

[26] Saha, U., Devan, K. and Ganesan, S. (2018) ‘A study to compute integrated dpa for neutron and ion irradiation environments using SRIM-2013’, Journal of Nuclear Materials, 503, pp. 30–39.

[27] Malo, S., Giroux, E., Araque Camacho, N., Chikada, T. and Tanaka, S. (2022) ‘Deuterium permeation through vanadium: Experimental determination and literature synthesis’, Membranes, 12(6), 579. doi:10.3390/membranes12060579.

[28] Su, X., Qin, X., Chen, D. and Li, Y. (2020) ‘First-principles study of hydrogen bubble nucleation in vanadium’, Materials, 13(2), 322. doi:10.3390/ma13020322.

[29] Kaletta, D. (1976) 'Helium-induced blistering in vanadium and vanadium-titanium alloys', Journal of Nuclear Materials, 63(3), pp. 347–355.

[30] Miyazawa, T., Tanaka, K., Hasegawa, A., Noda, K., Abe, K. and Muroga, T. (2014) 'Evaluation of irradiation hardening of ion-irradiated V–4Cr–4Ti and V–4Cr–4Ti–0.15Y alloys by nanoindentation techniques', Journal of Nuclear Materials, 455(1–3), pp. 440–444. doi:10.1016/j.jnucmat.2014.07.059.

[31] Loomis, B.A., Diercks, D.R. and Chung, H.M. (1995) 'Tensile properties of V–4Cr–4Ti after neutron irradiation to high doses', Fusion Engineering and Design, 29, pp. 399–405. doi:10.1016/0920-3796(95)80053-Z.

[32] Kiener, D., Grosinger, W., Dehm, G. and Pippan, R. (2011) 'Nano-compression testing of proton-irradiated single-crystal copper', Nature Materials, 10, pp. 608–613. doi:10.1038/nmat3055.

[33] Sznajder, M., Geppert, U. and Dudek, M.R. (2018) 'Hydrogen blistering under extreme radiation conditions', npj Materials Degradation, 2, 3. doi:10.1038/s41529-017-0024-z.

[34] Serafim, C., Calatroni, S., Djurabekova, F. and Peacock, R. (2025) 'Effects of low beam irradiation and high field pulsing tests in different metals', Physical Review Accelerators and Beams, 28, 013101. doi:10.1103/PhysRevAccelBeams.28.013101.

[35] Qadr, M.R. (2020) 'Effect of ion irradiation on the mechanical properties of high and low copper', Atom Indonesia, 46(2), pp. 119–124. doi:10.17146/aij.2020.923.

[36] Iwamoto, Y., Meigo, S. and Hashimoto, S. (2020) 'Estimation of reliable displacements-per-atom based on athermal-recombination-corrected model in radiation environments', Journal of Nuclear Materials, 538, 152261.

[37] Stoller, R.E., Toloczko, M.B., Was, G.S., Certain, A.G., Dwaraknath, S. and Garner, F.A. (2013) 'On the use of SRIM for computing radiation damage exposure', Nuclear Instruments and Methods in Physics Research Section B, 310, pp. 75–80. doi:10.1016/j.nimb.2013.05.008.

[38] Ziegler, J.F., Ziegler, M.D. and Biersack, J.P. (2010) 'SRIM – The stopping and range of ions in matter', Nuclear Instruments and Methods in Physics Research Section B, 268(11–12), pp. 1818–1823. doi:10.1016/j.nimb.2010.02.091.

[39] Norgett, M.J., Robinson, M.T. and Torrens, I.M. (1975) 'A proposed method of calculating displacement dose rates', Nuclear Engineering and Design, 33(1), pp. 50–54. doi:10.1016/0029-5493(75)90035-7.

[40] Kinchin, G.H. and Pease, R.S. (1955) 'The displacement of atoms in solids by radiation', Reports on Progress in Physics, 18(1), pp. 1–51. doi:10.1088/0034-4885/18/1/301.

[41] Nordlund, K., Zinkle, S.J., Sand, A.E., Granberg, F., Averback, R.S., Stoller, R.E., Suzudo, T., Malerba, L., Banhart, F., Weber, W.J., Willaime, F., Dudarev, S.L. and Simeone, D. (2018) 'Primary radiation damage: A review of current understanding and models', Journal of Nuclear Materials, 512, pp. 450–479. doi:10.1016/j.jnucmat.2018.10.027.

[42] Konobeyev, A.Yu., Fischer, U., Korovin, Yu.A. and Simakov, S.P. (2017) 'Evaluation of effective threshold displacement energies and other data required for the calculation of advanced atomic displacement cross-sections', Nuclear Energy and Technology, 3(3), pp. 169–175. doi:10.1016/j.nucet.2017.08.007.

[43] Serafim, C., Calatroni, S., Djurabekova, F. and Peacock, R. (2025) 'Effects of low beam irradiation and high field pulsing tests in different metals', Physical Review Accelerators and Beams, 28, 013101. doi:10.1103/PhysRevAccelBeams.28.013101.

[44] Sznajder, M., Geppert, U. and Dudek, M.R. (2018) 'Hydrogen blistering under extreme radiation conditions', npj Materials Degradation, 2, Article 3. doi:10.1038/s41529-017-0024-z.

[45] Kiener, D., Grosinger, W., Dehm, G. and Pippan, R. (2011) 'A further step towards an understanding of size-dependent crystal plasticity: Nano-compression testing of proton-irradiated single-crystal copper', Nature Materials, 10, pp. 608–613. doi:10.1038/nmat3055.

[46] Farrell, K. and King, J.E. (1988) ‘Defect structure development in 14 MeV neutron irradiated copper and copper dilute alloys’, Journal of Nuclear Materials, 155–157, pp. 443–450. doi:10.1016/0022-3115(88)90287-5.

[47] Loomis, B.A., Diercks, D.R. and Chung, H.M. (1995) ‘Tensile properties of V–4Cr–4Ti after neutron irradiation to high doses’, Fusion Engineering and Design, 29, pp. 399–405. doi:10.1016/0920-3796(95)80053-Z.

[48] Ryabov, V.A. and Fedorov, A.A. (2000) ‘Features of radiation damage of vanadium and its alloys at a temperature of 330–340 °C’, Journal of Nuclear Materials, 285, pp. 35–42. doi:10.1016/S0022-3115(00)00218-X.

[49] Nordlund, K., Sand, A.E., Granberg, F., Zinkle, S.J. and Stoller, R.E. (2015) Primary radiation damage in materials: Review of current understanding and proposed new standard displacement damage model. OECD Nuclear Energy Agency, NEA/NSC/DOC(2015)9.

[50] Ophoven, N., Mauerhofer, E., Li, J., Rücker, U., Zakalek, P., Baggemann, J., Gutberlet, T., Brückel, T. and Langer, C. (2021) ‘Monte Carlo simulation of proton- and neutron-induced radiation damage in a tantalum target irradiated by 70 MeV protons’, Applied Physics A, 127, Article 576. doi:10.1007/s00339-021-04713-4.

[51] Zinkle, S.J. and Was, G.S. (2013) ‘Materials challenges in nuclear energy’, Acta Materialia, 61(3), pp. 735–758. doi:10.1016/j.actamat.2012.11.004.

8 Appendices

8.1 Appendix A: SRIM Simulation Parameters Summary

Vanadium 20 MeV Proton Simulation:

• Ion: Hydrogen (H), Mass = 1.008 amu, Energy = 20 MeV

• Target: Vanadium, Mass = 50.9415 amu, Density = 6.11 g/cm^3

• Layer thickness: 3.7 mm

• Displacement energies: 46, 57, 68 eV

• Lattice binding energy: 0 eV (ASTM standard)

• Surface binding energy: 5.3 eV

• Number of ions: 15,000

• Calculation mode: Full damage cascades

Copper 3 MeV Proton Simulation:

• Ion: Hydrogen (H), Mass = 1.008 amu, Energy = 3 MeV

• Target: Copper, Mass = 63.546 amu, Density = 8.96 g/cm^3

• Layer thickness: 0.5 mm

• Displacement energies: 24, 30, 36 eV

• Lattice binding energy: 0 eV

• Surface binding energy: 3.5 eV

• Number of ions: 15,000

• Calculation mode: Full damage cascades

8.2 Appendix B: Damage Rate Calculation Examples

Case: Vanadium with Ed = 46 eV

Given:

• Displacements per ion (from SRIM): n = 70

• Proton flux: Φ = 0.011096 ions/s

• Atomic density: Na = 0.0722 atoms/Å^3

Damage rate:

$$Rd = (n \times \Phi) / Na = (70 \times 0.011096) / 0.0722 = 3.41 \times 10^{-7} \text{ dpa/s}$$

Annual damage (Full Power Year):

$\text{dpa/FPY} = 3.41 \times 10^{-7} \times 3.153 \times 10^{7} = 10.76$ dpa/FPY

Lifetime to 30 dpa:

Lifetime = 30 dpa / 10.76 dpa/FPY = 2.79 years

This corrected calculation shows that for the minimum displacement energy case (E_d = 46 eV), the vanadium target would accumulate 10.76 dpa per full power year, reaching the 30 dpa critical threshold in approximately 2.79 years of continuous operation.

Example: Copper with E_d = 30 eV (average case)

Given:

- Displacements per ion (from SRIM): n = 37
- Proton flux: $\Phi = 0.11889$ ions/s
- Atomic density: $N_a = 0.08453$ atoms/Å³

Damage rate:

$R_d = (n \times \Phi) / N_a = (37 \times 0.11889) / 0.08453 = 1.14 \times 10^{-6}$ dpa/s

Annual damage (Full Power Year):

$\text{dpa/FPY} = 1.14 \times 10^{-6} \times 3.153 \times 10^{7} = 36.03$ dpa/FPY

Lifetime to 5 dpa (embrittlement threshold):

Lifetime = 5 dpa / 36.03 dpa/FPY = 0.139 years = 51 days

8.3 Appendix C: Glossary of Technical Terms

- Arc-dpa: Athermal recombination-corrected displacement per atom
- BCA: Binary collision approximation
- Cascade: Sequence of atomic collisions initiated by energetic recoil
- dpa: Displacement per atom (unitless damage metric)

• Ed: Threshold displacement energy
• FPY: Full Power Year - standardized unit for annual damage accumulation assuming continuous operation
• Frenkel pair: Vacancy-interstitial defect pair
• HBS: High Brilliance neutron Source
• MD: Molecular dynamics simulation
• NRT: Norgett-Robinson-Torrens damage model
• PKA: Primary knock-on atom
• SRIM/TRIM: Stopping and Range of Ions in Matter / Transport of Ions in Matter
• TMR: Target-moderator-reflector unit
• Tdam: Damage energy available for displacement production